

Using Diamond Tiles for the Modular Design of Hexagonal Phased Arrays

P. Rocca, N. Anselmi, A. Polo, and A. Massa

Contents

1 Numerical Results	3
1.1 OTM - Integer - Hexagon (10,10,10) - Mask Matching - Steering $(\theta, \phi) = (30, 0)$ [deg] - Markov Init. $N_I = 542$	3
1.2 OTM - Binary vs. Integer - Hexagon (10,10,10) - Mask Matching - Broadside - $d_{y2} = 0.5\lambda$	10
1.3 OTM - Binary vs. Integer - Hexagon (10,10,10) - Mask Matching - Steering $(\theta, \phi) = (30, 0)$ [deg] - $d_{y2} = 0.5\lambda$	21
1.4 OTM - Integer - Hexagon (10,10,10) - Mask Matching - Broadside - $d_{y2} = 0.69\lambda$	28
2 Conclusions	37

1 Numerical Results

1.1 OTM - Integer - Hexagon (10,10,10) - Mask Matching - Steering $(\theta, \phi) = (30, 0)$ [deg] - Markov Init. $N_I = 542$

Array Geometry

Conclusion

The solution with OTM-GA [Sec. [sec: OTM sw update - case 20]] is a good choice respect to ETM for the same array architecture; because it is possible to obtain good results with less computational effort. The local minimum obtained on the fitness is worst than OTM-GA binary [Sec. [sec: OTM sw update - case 13]], but it is best than OTM-GA integer [Sec. [sec: OTM sw update - case 16]] with random population and OTM-GA integer [Sec. [sec: OTM sw update - case 18]] with population generated with Hidden Markov Model with population dimension of 272 individuals. In this test case there isn't convergence on the solution space on the fitness minimum. A possible solution to improve the results is to generate a new initial population by increasing the number of flips $\left\lfloor N_{\text{flips}} \right\rfloor$.

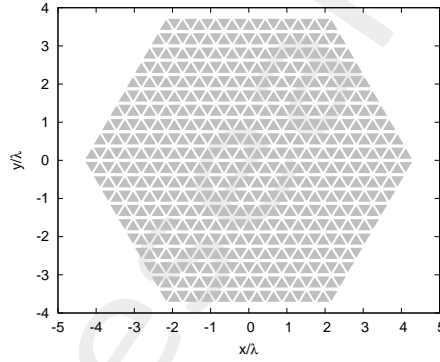


Figure 1: $N_{\text{tot}} = 600$, $L_d = 20\lambda$, $d_x = 0.22\lambda$, $d_{y1} = 0.25\lambda$, $d_{y2} = 0.5\lambda$, $N_c^{\text{tot}} = 800$, $N_p^{\text{tot}} = 441$, $N_p^{(\text{bound})} = 61$, $a = 10$, $b = 10$, $c = 10$ – Array Geometry

Reference Array, Convex Programming Excitations

Test case parameters

- Number of array elements - $N_{\text{tot}} = 600$
- Element spacing along x - $d_x = 0.22\lambda$
- Element spacing along y_1 - $d_{y1} = 0.25\lambda$
- Element spacing along y_2 - $d_{y2} = 0.5\lambda$
- Pointing Direction - $\theta_0 = 30^\circ$
- Pointing Direction - $\phi_0 = 0^\circ$
- Pointing Direction - $u_0 = 0.5$

- Pointing Direction - $v_0 = 0$
- A side length - $a = 10$
- B side length - $b = 10$
- C side length - $c = 10$

Mask Constraints

The following mask (Fig.2) is used to calculate the fitness function.

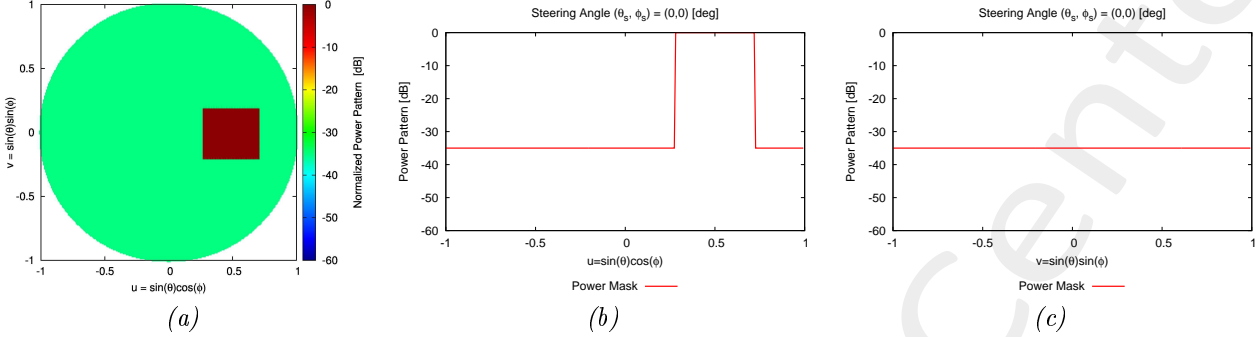


Figure 2: Mask Power Pattern in broadside direction $(\theta, \phi) = (30, 0)$ [deg]: (a) 2D, (b) Normalized cut along azimuth direction, (c) Normalized cut along elevation direction.

Array Tiling

Software Parameters

- Number of array elements - $N_{tot} = 600$
- Element spacing along x - $d_x = 0.22\lambda$
- Element spacing along y_1 - $d_{y1} = 0.25\lambda$
- Element spacing along y_2 - $d_{y2} = 0.5\lambda$
- Side's domain - $L_d = 20\lambda$
- Points number - $N_p^{tot} = 441$
- Points along x - $M_p = 21$
- Points along y - $N_p = 21$
- Total cells number - $N_c^{tot} = 800$
- Cells along x - $M_c = 40$
- Cells along y - $N_c = 20$
- Boundary points - $N_p^{(bound)} = 61$
- Samples along u - $N_u = 256$
- Samples along v - $N_v = 256$
- SLL weight - $w_{SLL} = 0.0$
- Directivity weight - $w_D = 0$

- HPBW weight azimuth - $w_{HPBW}^{azm} = 0.0$
- HPBW weight elevation - $w_{HPBW}^{elv} = 0.0$
- Mask weight - $w_{mask} = 1.0$
- Cell elements - $N_{el} = 1$
- Pointing Direction - $\theta_0 = 30^\circ$
- Pointing Direction - $\phi_0 = 0^\circ$
- Pointing Direction - $u_0 = 0.5$
- Pointing Direction - $v_0 = 0$
- A side length - $a = 10$
- B side length - $b = 10$
- C side length - $c = 10$
- A side length in λ - $L_a = 4.33\lambda$
- B side length in λ - $L_b = 4.33\lambda$
- C side length in λ - $L_c = 4.33\lambda$
- Tiling configurations - $T = 9.27 \times 10^{33}$
- Number of unknowns - $N_u = 271$
- Maximum of word max - $U_{max} = 10$
- Number of trials (seed) - $N_{seed} = 105$
- Number of individuals - $N_I = 542$
- Number of flips - $N_{flips} = 500$
- Cross-Over probability - $p_{cx} = 0.9$
- Mutation probability - $p_m = 0.001$

Results

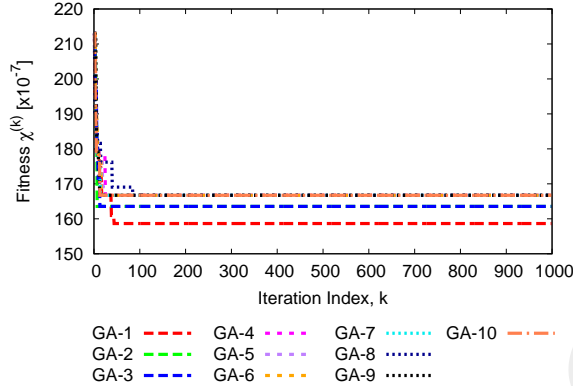


Figure 3: Fitness for 10 best seeds

GA	Seed	SLL [dB]	HPBW (az) [deg]	HPBW (el) [deg]	D [dB]	Fitness Value
1	0.551	-33.669	8.996	8.928	26.774	1.587×10^{-5}
2	0.326	-33.675	8.996	8.928	26.773	1.636×10^{-5}
3	0.35	-33.675	8.996	8.928	26.773	1.636×10^{-5}
4	0.051	-33.739	8.997	8.929	26.773	1.667×10^{-5}
5	0.073	-33.739	8.997	8.929	26.773	1.667×10^{-5}
6	0.0	-33.739	8.997	8.929	26.773	1.667×10^{-5}
7	0.157	-33.739	8.997	8.929	26.773	1.667×10^{-5}
8	0.15	-33.739	8.997	8.929	26.773	1.667×10^{-5}
9	0.259	-33.739	8.997	8.929	26.773	1.667×10^{-5}
10	0.284	-33.739	8.997	8.929	26.773	1.667×10^{-5}

Table 3: Solution Parameters of Radiation Pattern along $(\theta_0, \phi_0) = (30, 0)$ [deg]

Fig. 3 represents the fitness value for 10 best seeds.

I analyzed the solution (seed) that permits to reach the minimum fitness value. The fitness analized corresponds to $seed = \{0.551\}$

Broadside Analysis

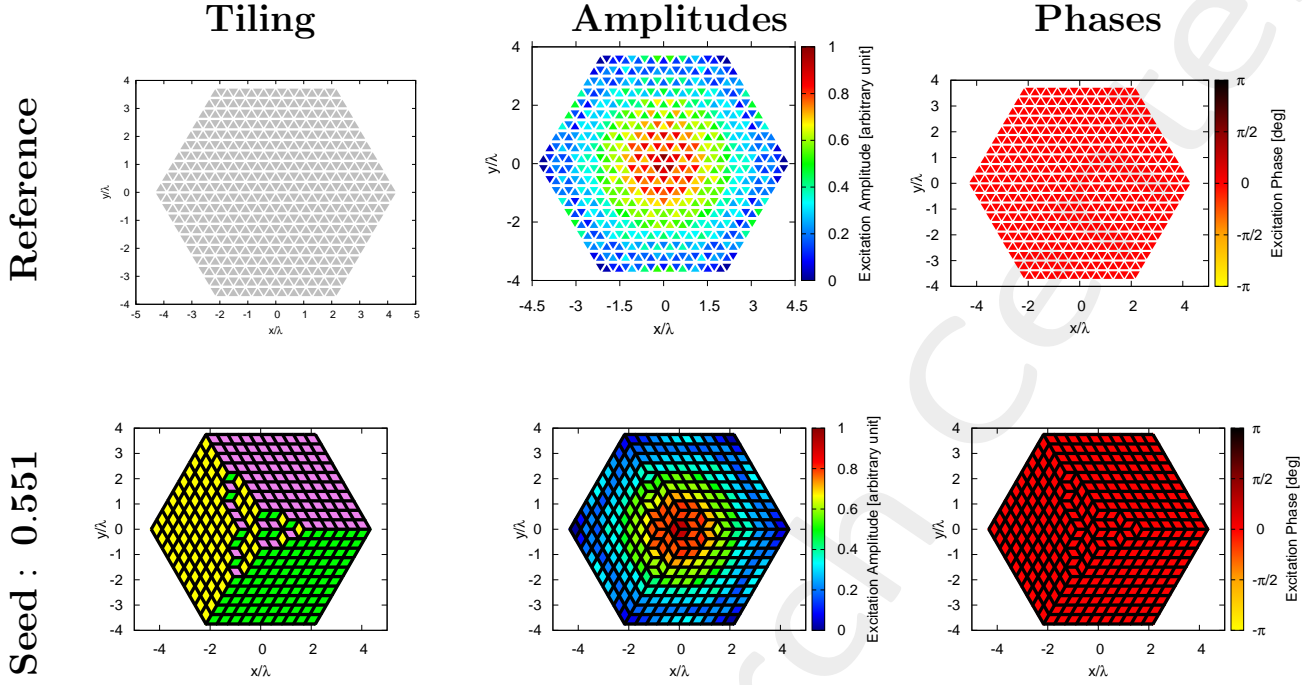


Figure 4: *Mask Matching*, $SLL = -34.79$ [dB], $N_{tot} = 600$, $L_d = 20\lambda$, $d_x = 0.22\lambda$, $d_{y1} = 0.25\lambda$, $d_{y2} = 0.5\lambda$, $a = 10$, $b = 10$, $c = 10$, $(\theta_0, \phi_0) = (0, 0)$ [deg] – Solution ID.: Reference, Seed 0.551

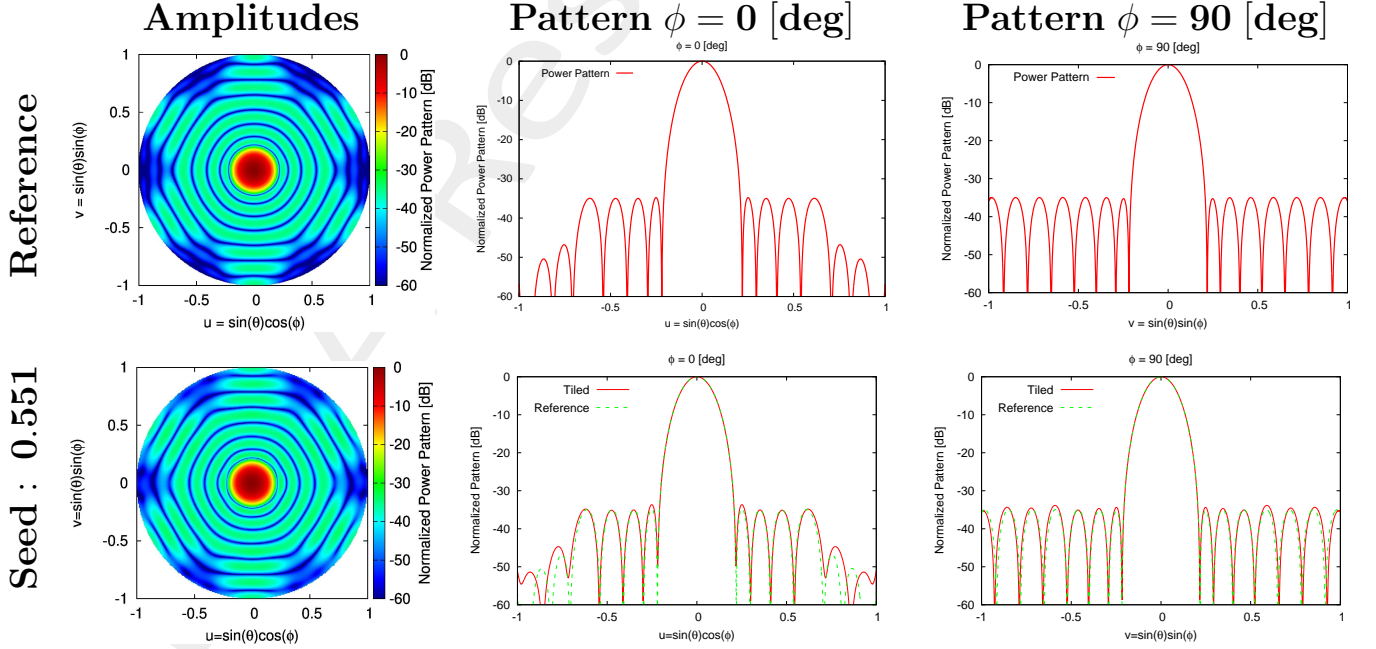


Figure 5: *Mask Matching*, $SLL = -34.79$ [dB], $N_{tot} = 600$, $L_d = 20\lambda$, $d_x = 0.22\lambda$, $d_{y1} = 0.25\lambda$, $d_{y2} = 0.5\lambda$, $a = 10$, $b = 10$, $c = 10$, $(\theta_0, \phi_0) = (0, 0)$ [deg] – Solution ID.: Reference, Seed 0.551

Steering Analysis

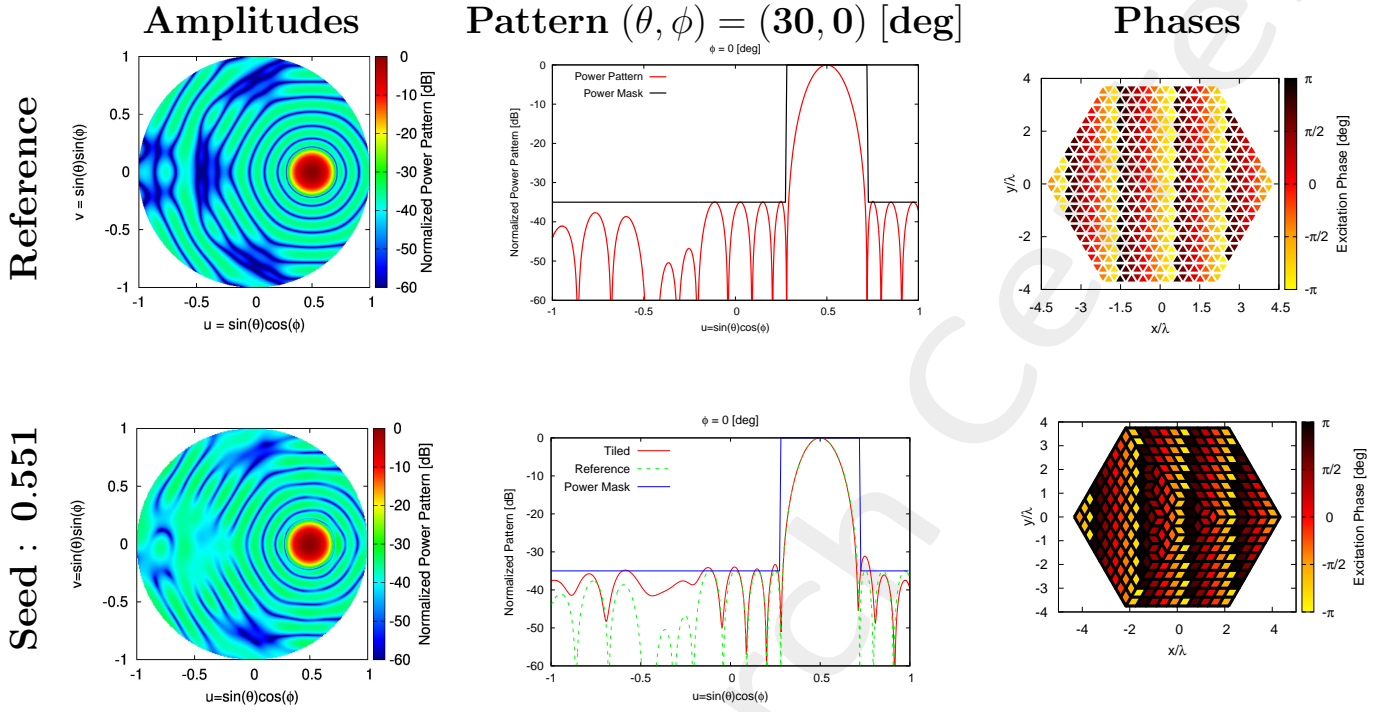


Figure 6: *Mask Matching*, $SLL = -34.79$ [dB], $N_{tot} = 600$, $L_d = 20\lambda$, $d_x = 0.22\lambda$, $d_{y1} = 0.25\lambda$, $d_{y2} = 0.5\lambda$, $a = 10$, $b = 10$, $c = 10$, $(\theta_0, \phi_0) = (30, 0)$ [deg] – Solution ID.: Reference, Seed 0.551

Solutions Summary

(a, b, c)	MAX_ITE (# iterations)	$\Delta\tau$ [sec] (single simulation period)	τ [sec] total simulation period
10, 10, 10	1000	0.108660	108.660

Table 7: Simulation Time

SOLUTION ID	SLL [dB]	HPBW (azimuth) [deg]	HPBW (elevation) [deg]	D [dB]	Mask Fitting
Reference	-34.788	10.415	8.914	26.132	0
Seed 0.551	-33.669	8.996	8.928	26.774	1.587×10^{-5}

Table 8: SLL , $HPBW_{az}$, $HPBW_{el}$, D , $Mask$ $Fitting$ of Radiation Pattern along $(\theta_0, \phi_0) = (30, 0)$ [deg]

1.2 OTM - Binary vs. Integer - Hexagon (10,10,10) - Mask Matching - Broadside

- $d_{y2} = 0.5\lambda$

Array Geometry

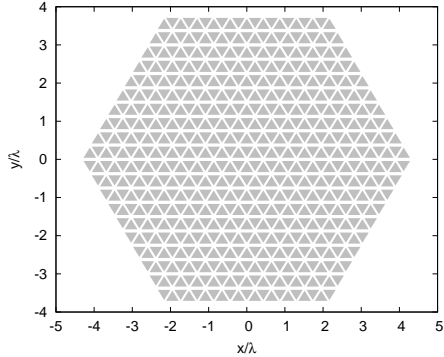


Figure 7: $N_{tot} = 600$, $L_d = 20\lambda$, $d_x = 0.22\lambda$, $d_{y1} = 0.25\lambda$, $d_{y2} = 0.5\lambda$, $N_c^{tot} = 800$, $N_p^{tot} = 441$, $N_p^{(bound)} = 61$, $a = 10$, $b = 10$, $c = 10$ – Array Geometry

Reference Array, Convex Programming Excitations

Test case parameters

- Number of array elements - $N_{tot} = 600$
- Element spacing along x - $d_x = 0.22\lambda$
- Element spacing along y_1 - $d_{y1} = 0.25\lambda$
- Element spacing along y_2 - $d_{y2} = 0.5\lambda$
- Pointing Direction - $\theta_0 = 0^\circ$
- Pointing Direction - $\phi_0 = 0^\circ$
- Pointing Direction - $u_0 = 0$
- Pointing Direction - $v_0 = 0$
- A side length - $a = 10$
- B side length - $b = 10$
- C side length - $c = 10$

Mask Constraints

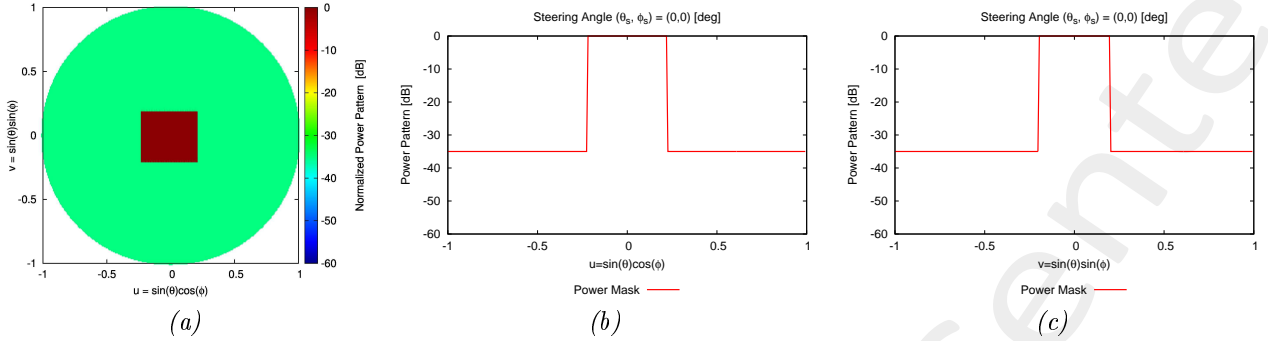


Figure 8: Mask Power Pattern in broadside direction $(\theta, \phi) = (0, 0)$ [deg]: (a) 2D, (b) Normalized cut along azimuth direction, (c) Normalized cut along elevation direction.

Array Tiling

Software Parameters

- Number of array elements - $N_{tot} = 600$
- Element spacing along x - $d_x = 0.22\lambda$
- Element spacing along y_1 - $d_{y1} = 0.25\lambda$
- Element spacing along y_2 - $d_{y2} = 0.5\lambda$
- Side's domain - $L_d = 20\lambda$
- Points number - $N_p^{tot} = 441$
- Points along x - $M_p = 21$
- Points along y - $N_p = 21$
- Total cells number - $N_c^{tot} = 800$
- Cells along x - $M_c = 40$
- Cells along y - $N_c = 20$
- Boundary points - $N_p^{(bound)} = 61$
- Samples along u - $N_u = 256$
- Samples along v - $N_v = 256$
- SLL weight - $w_{SLL} = 0.0$
- Directivity weight - $w_D = 0$

- HPBW weight azimuth - $w_{HPBW}^{azm} = 0.0$
- HPBW weight elevation - $w_{HPBW}^{elv} = 0.0$
- Mask weight - $w_{mask} = 1.0$
- Cell elements - $N_{el} = 1$
- Pointing Direction - $\theta_0 = 0^\circ$
- Pointing Direction - $\phi_0 = 0^\circ$
- Pointing Direction - $u_0 = 0$
- Pointing Direction - $v_0 = 0$
- A side length - $a = 10$
- B side length - $b = 10$
- C side length - $c = 10$
- A side length in λ - $L_a = 4.33\lambda$
- B side length in λ - $L_b = 4.33\lambda$
- C side length in λ - $L_c = 4.33\lambda$
- Tiling configurations - $T = 9.27 \times 10^{33}$
- Number of unknowns - $N_u = 1084$
- Maximum of word max - $U_{max} = 10$
- Number of trials (seed) - $N_{seed} = 99$
- Cross-Over probability - $p_{cx} = 0.9$
- Mutation probability - $p_m = 0.001$

Results

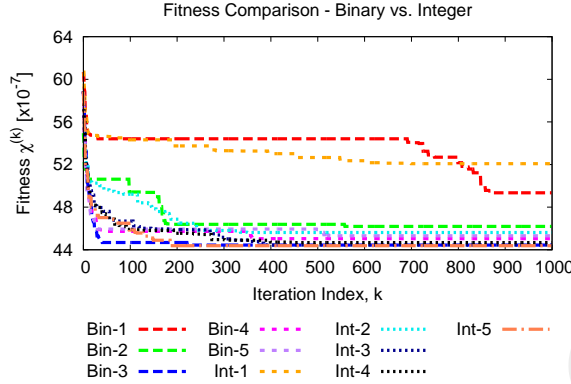


Figure 9: Best 10 fitness for binary and integer coding for the same initial population

The meaning of labels in Fig.9 is stated in Tab.11.

Label	Coding	Population Type	N_I	N_{flips}
Bin - 1	Binary	Analytical	272	/
Bin - 2	Binary	Markov	272	200
Bin - 3	Binary	Markov	542	500
Bin - 4	Binary	Markov	272	1×10^5
Bin - 5	Binary	Markov	542	1×10^5
Int - 1	Integer	Analytical	272	/
Int - 2	Integer	Markov	272	200
Int - 3	Integer	Markov	542	500
Int - 4	Integer	Markov	272	1×10^5
Int - 5	Integer	Markov	542	1×10^5

Table 11: Legend of label in Fig.9.

Label	Minimum	Maximum	Average	Variance
Bin - 1	4.935×10^{-6}	5.518×10^{-6}	5.365×10^{-6}	1.179×10^{-14}
Bin - 2	4.619×10^{-6}	5.201×10^{-6}	5.015×10^{-6}	9.156×10^{-15}
Bin - 3	4.444×10^{-6}	5.042×10^{-6}	4.703×10^{-6}	2.433×10^{-14}
Bin - 4	4.505×10^{-6}	5.044×10^{-6}	4.775×10^{-6}	1.019×10^{-14}
Bin - 5	4.532×10^{-6}	4.971×10^{-6}	4.699×10^{-6}	8.307×10^{-15}
Int - 1	5.208×10^{-6}	5.519×10^{-6}	5.383×10^{-6}	7.680×10^{-15}
Int - 2	4.562×10^{-6}	5.215×10^{-6}	5.048×10^{-6}	1.211×10^{-14}
Int - 3	4.444×10^{-6}	5.118×10^{-6}	4.803×10^{-6}	2.946×10^{-14}
Int - 4	4.468×10^{-6}	5.122×10^{-6}	4.727×10^{-6}	2.585×10^{-14}
Int - 5	4.438×10^{-6}	5.123×10^{-6}	4.680×10^{-6}	2.483×10^{-14}

Table 12: Statistics of all fitness in Fig.9

Fig. 9 rappresents the best fitness value for binary and integer case for 5 different initial populations.

I analyzed the solution that permits to reach the minimum fitness value, associated with the minimum average value. The fitness to analize is $Int - 5$.

The parameters for this test case are:

- Number of individuals - $N_I = 542$
- Number of flips - $N_{flips} = 1 \times 10^5$
- Coding Type - Integer

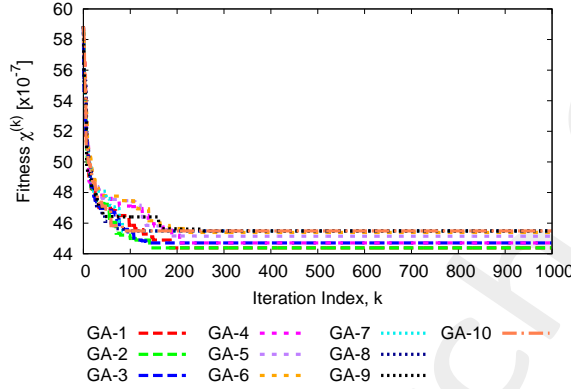


Figure 10: Fitness for 10 best seeds

GA	Seed	SLL [dB]	HPBW (az) [deg]	HPBW (el) [deg]	D [dB]	Fitness Value
1	0.284	-33.714	8.997	8.928	26.773	4.438×10^{-6}
2	0.95	-33.714	8.997	8.928	26.773	4.438×10^{-6}
3	0.225	-33.684	8.997	8.928	26.773	4.47×10^{-6}
4	0.936	-33.684	8.997	8.928	26.773	4.47×10^{-6}
5	0.514	-33.646	8.997	8.927	26.773	4.514×10^{-6}
6	0.903	-33.649	8.997	8.927	26.773	4.539×10^{-6}
7	0.445	-33.674	8.997	8.928	26.773	4.548×10^{-6}
8	0.126	-33.572	8.996	8.927	26.774	4.549×10^{-6}
9	0.15	-33.572	8.996	8.927	26.774	4.549×10^{-6}
10	0.188	-33.572	8.996	8.927	26.774	4.549×10^{-6}

Table 14: Solution Parameters of Radiation Pattern along $(\theta_0, \phi_0) = (0, 0)$ [deg]

Fig.10 rappresents the fitness value for 10 best seeds.

I analyzed the solution (seed) that permits to reach the minimum fitness value. The solutions analized corresponds to $seed = \{0.284, 0.95\}$.

Best Individuals

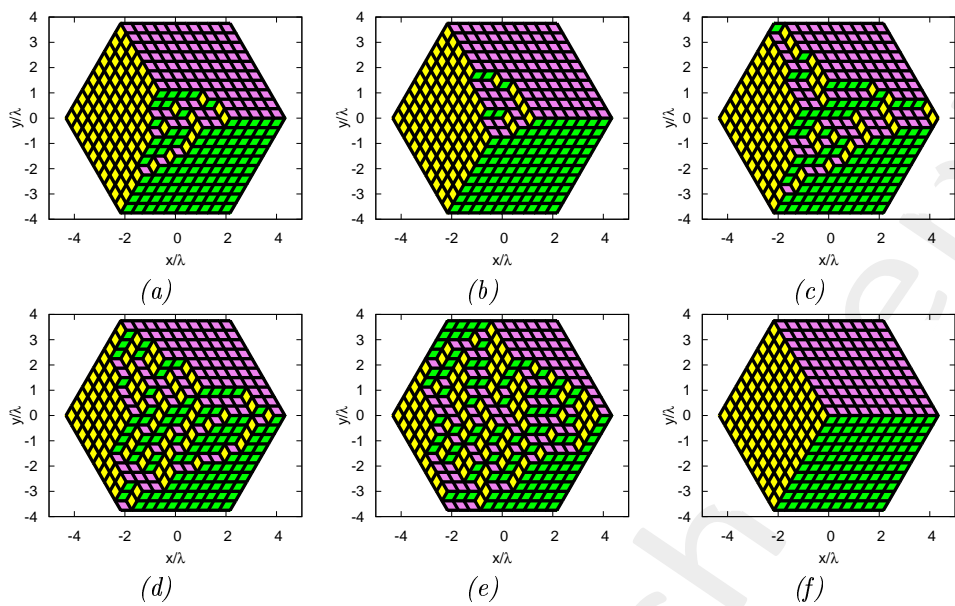


Figure 11: Best individuals of initial population: (a) Individual nr. 7, (b) Individual nr. 26, (c) Individual nr. 55, (d) Individual nr. 145, (e) Individual nr. 185, (f) Individual nr. 292.

Broadside Analysis

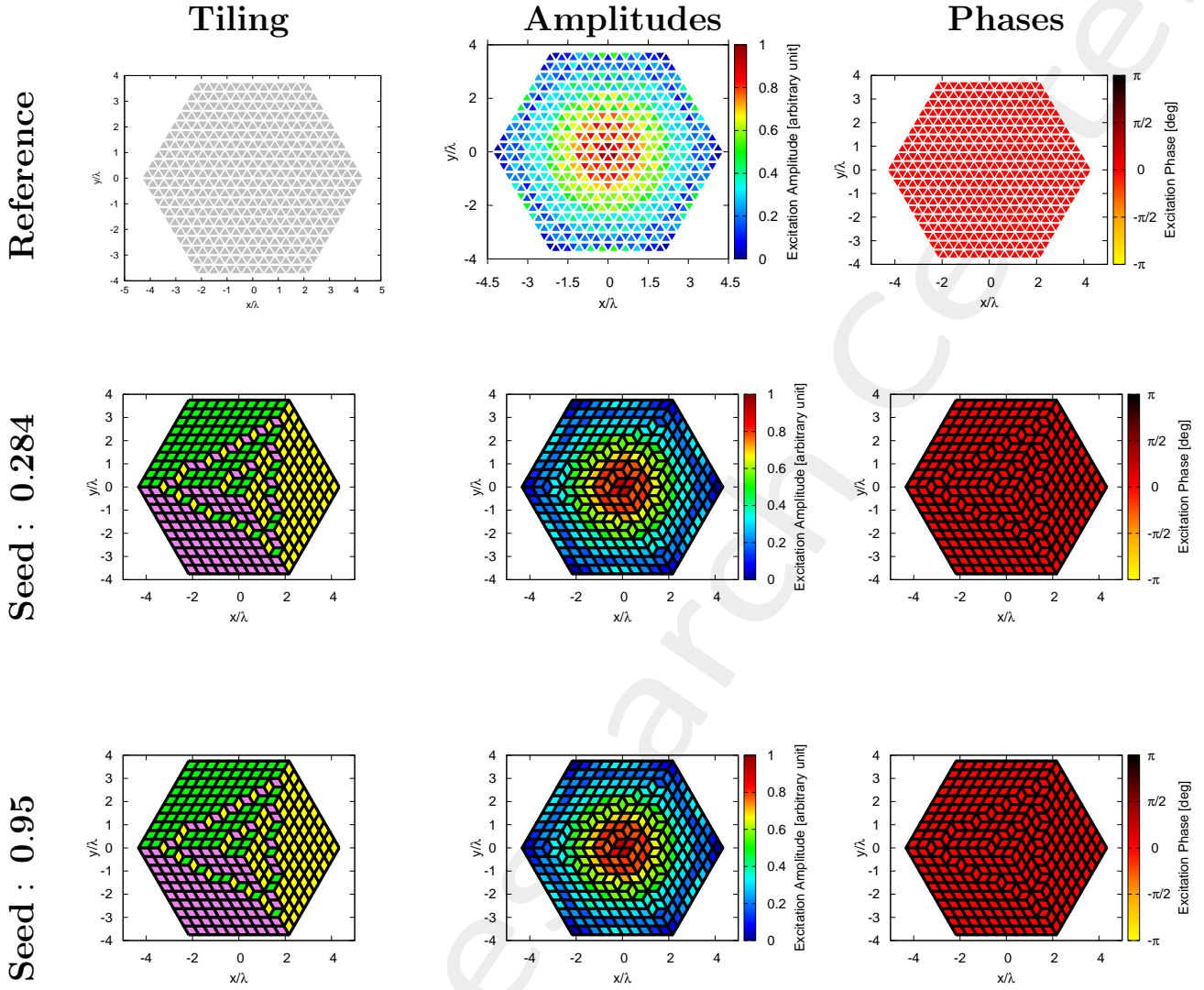


Figure 12: *Mask Matching*, $SLL = -34.79$ [dB], $N_{tot} = 600$, $L_d = 20\lambda$, $d_x = 0.22\lambda$, $d_{y1} = 0.25\lambda$, $d_{y2} = 0.5\lambda$, $a = 10$, $b = 10$, $c = 10$, $(\theta_0, \phi_0) = (0, 0)$ [deg] – Solution ID.: Reference, Seed 0.284, Seed 0.95

The best solutions have the same tiling configuration, so the radiation properties are the same, so I analyze only the solutions with $seed = \{0.284\}$.

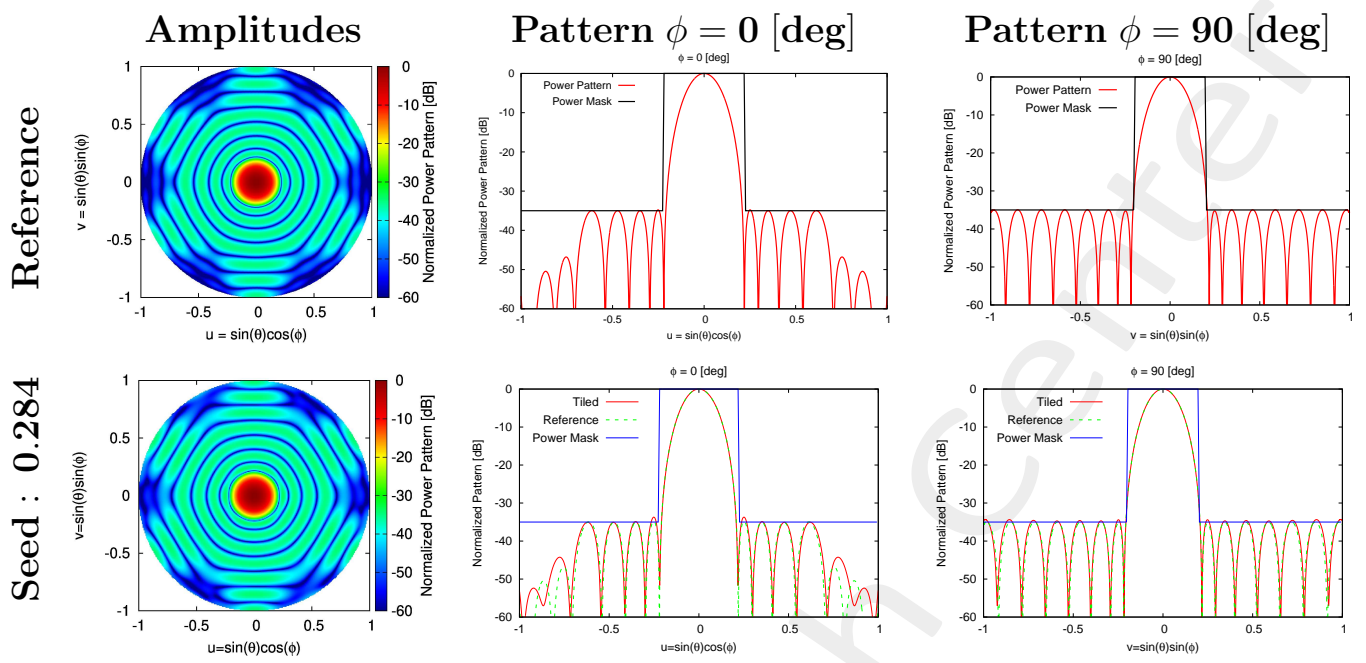


Figure 13: *Mask Matching*, $SLL = -34.79$ [dB], $N_{tot} = 600$, $L_d = 20\lambda$, $d_x = 0.22\lambda$, $d_{y1} = 0.25\lambda$, $d_{y2} = 0.5\lambda$, $a = 10$, $b = 10$, $c = 10$, $(\theta_0, \phi_0) = (0, 0)$ [deg] – Solution ID.: Reference, Seed 0.284

Steering Analysis

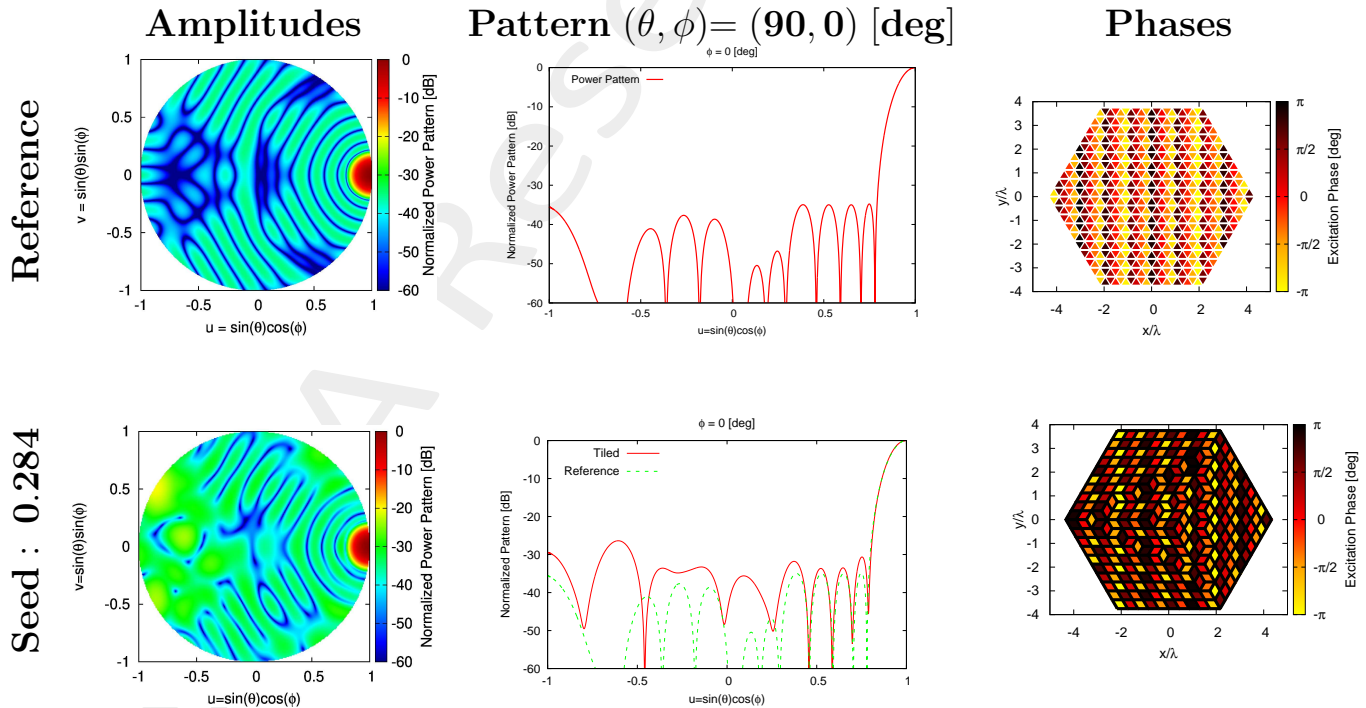


Figure 14: *Mask Matching*, $SLL = -34.79$ [dB], $N_{tot} = 600$, $L_d = 20\lambda$, $d_x = 0.22\lambda$, $d_{y1} = 0.25\lambda$, $d_{y2} = 0.5\lambda$, $a = 10$, $b = 10$, $c = 10$, $(\theta_0, \phi_0) = (90, 0)$ [deg] – Solution ID.: Reference, Seed 0.284

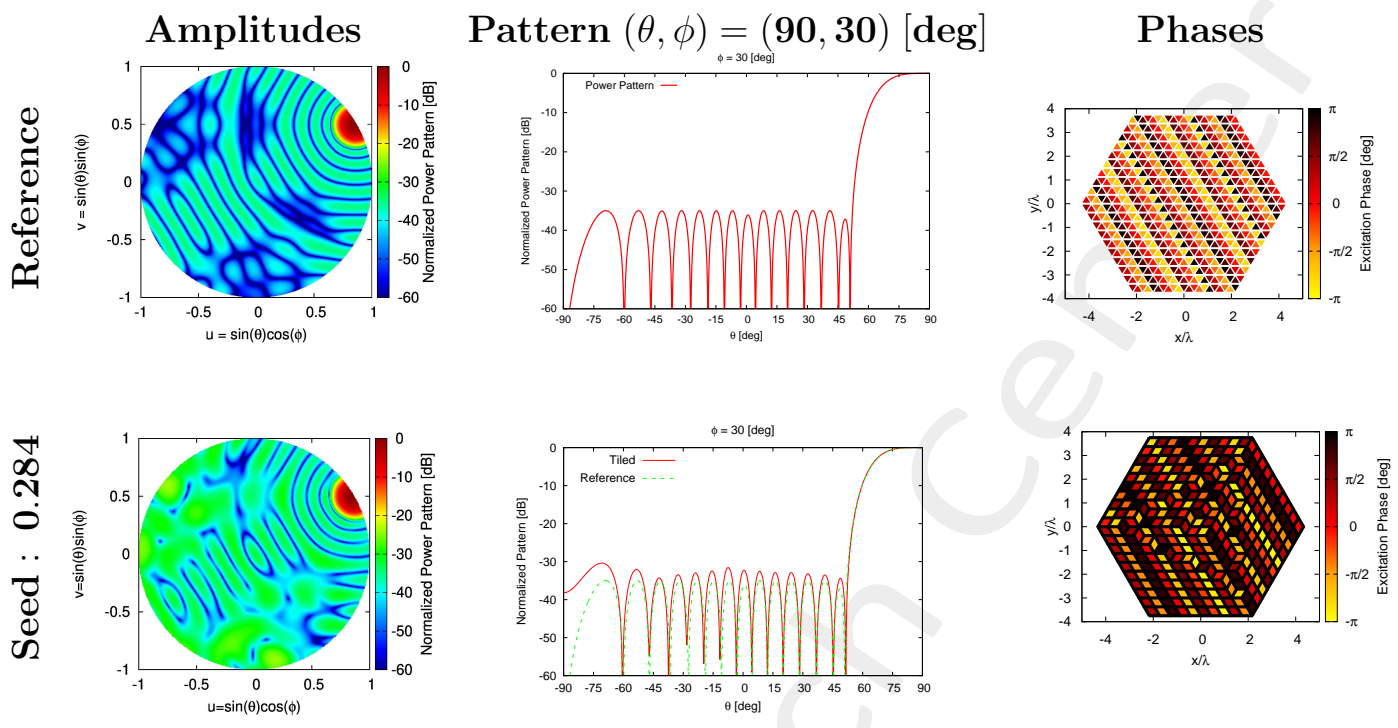


Figure 15: *Mask Matching*, $SLL = -34.79$ [dB], $N_{tot} = 600$, $L_d = 20\lambda$, $d_x = 0.22\lambda$, $d_{y1} = 0.25\lambda$, $d_{y2} = 0.5\lambda$, $a = 10$, $b = 10$, $c = 10$, $(\theta_0, \phi_0) = (90, 30)$ [deg] – Solution ID.: Reference, Seed 0.284

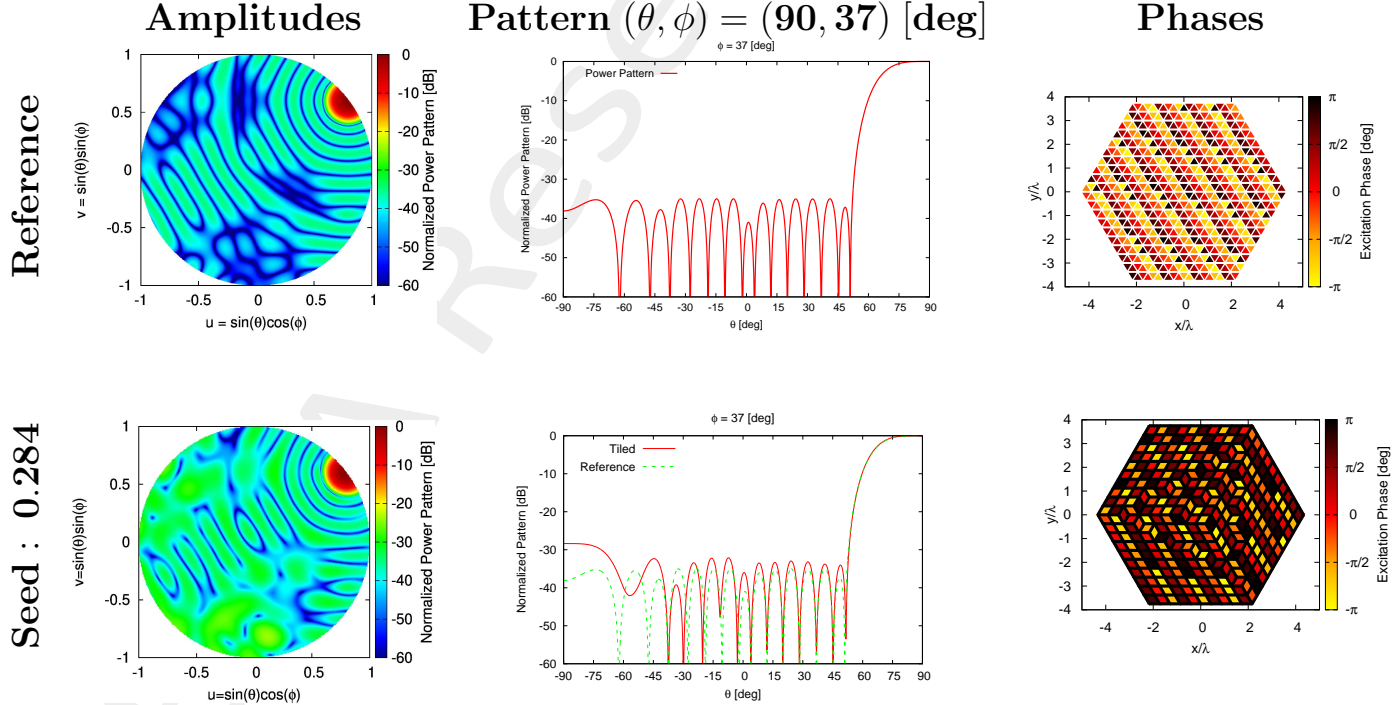


Figure 16: *Mask Matching*, $SLL = -34.79$ [dB], $N_{tot} = 600$, $L_d = 20\lambda$, $d_x = 0.22\lambda$, $d_{y1} = 0.25\lambda$, $d_{y2} = 0.5\lambda$, $a = 10$, $b = 10$, $c = 10$, $(\theta_0, \phi_0) = (90, 37)$ [deg] – Solution ID.: Reference, Seed 0.284

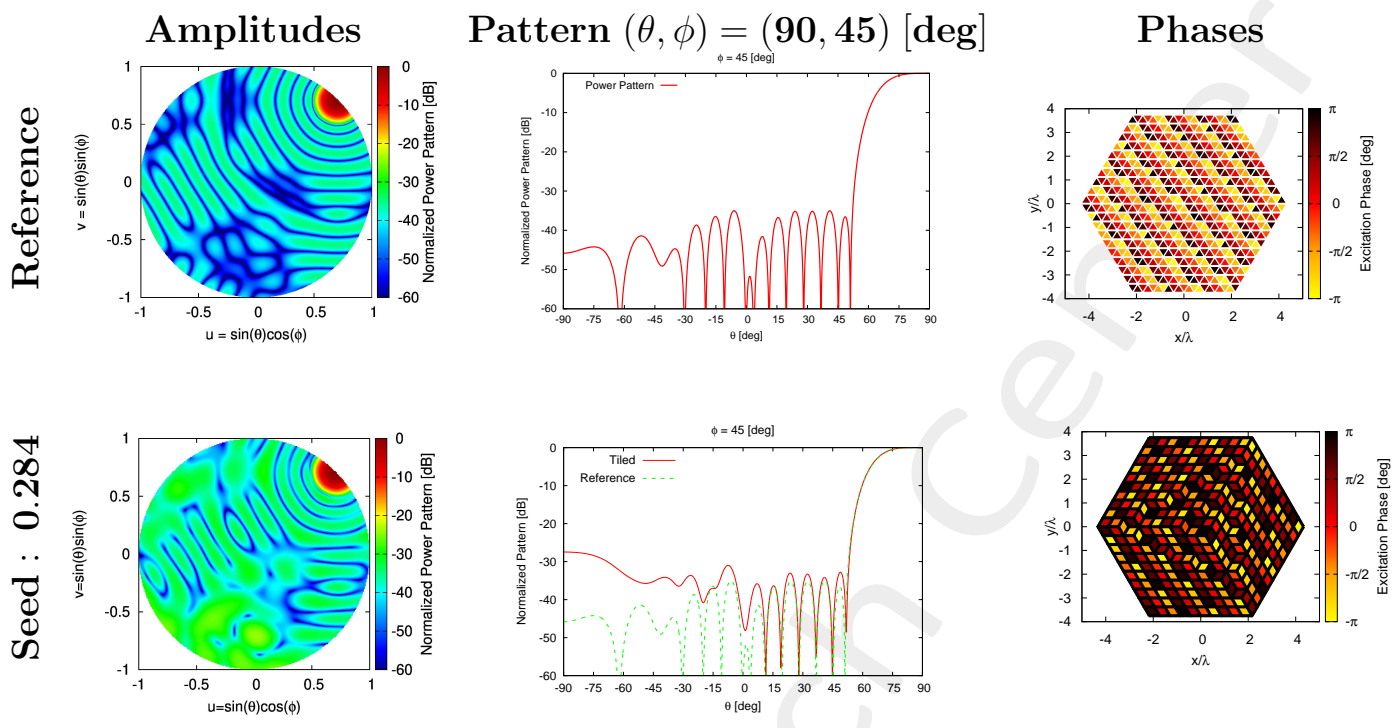


Figure 17: *Mask Matching*, $SLL = -34.79$ [dB], $N_{tot} = 600$, $L_d = 20\lambda$, $d_x = 0.22\lambda$, $d_{y1} = 0.25\lambda$, $d_{y2} = 0.5\lambda$, $a = 10$, $b = 10$, $c = 10$, $(\theta_0, \phi_0) = (90, 45)$ [deg] – Solution ID.: Reference, Seed 0.284

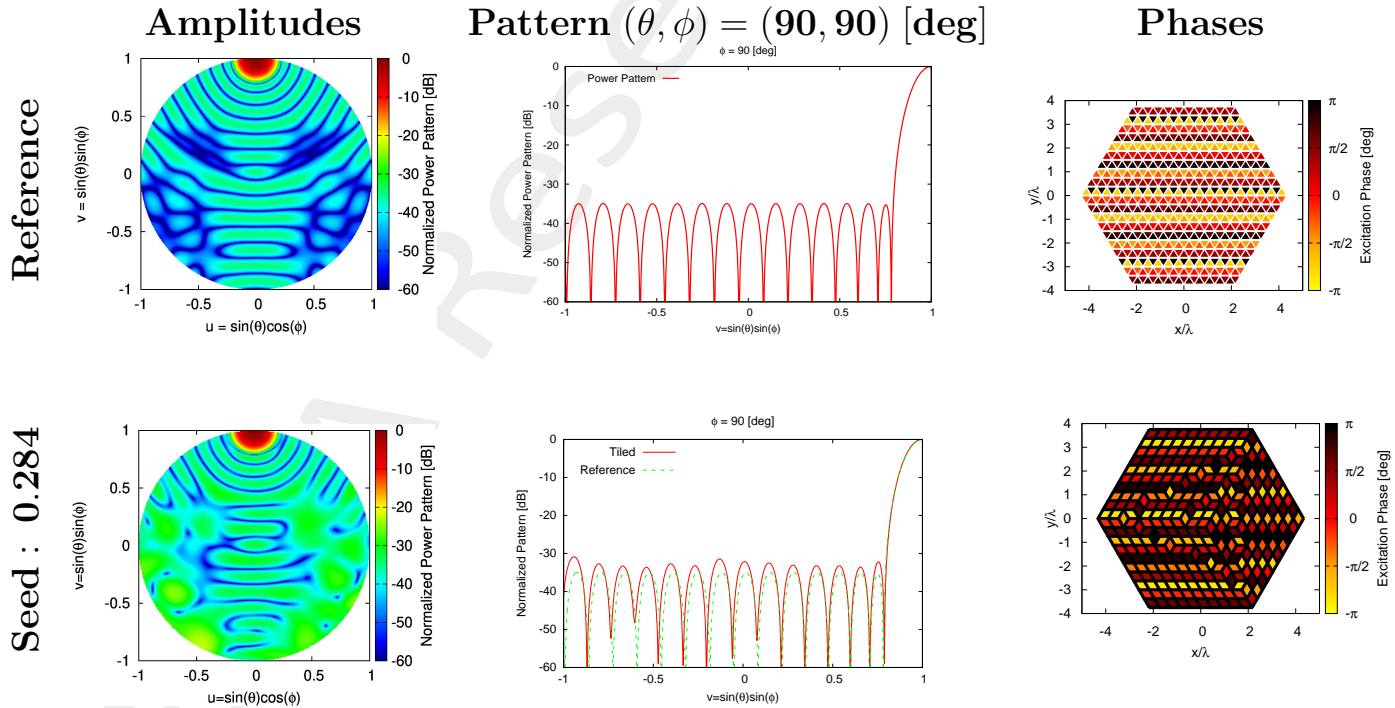


Figure 18: *Mask Matching*, $SLL = -34.79$ [dB], $N_{tot} = 600$, $L_d = 20\lambda$, $d_x = 0.22\lambda$, $d_{y1} = 0.25\lambda$, $d_{y2} = 0.5\lambda$, $a = 10$, $b = 10$, $c = 10$, $(\theta_0, \phi_0) = (90, 90)$ [deg] – Solution ID.: Reference, Seed 0.284

Solutions Summary

(a, b, c)	MAX_ITE (# iterations)	$\Delta\tau$ [sec] (single simulation period)	τ [sec] total simulation period
10, 10, 10	1000	0.191937	191.937

Table 23: Simulation Time

SOLUTION ID	SLL [dB]	HPBW (azimuth) [deg]	HPBW (elevation) [deg]	D [dB]	Mask Fitting
Reference	-34.788	9.003	8.914	26.791	0
Seed 0.284	-33.714	8.997	8.928	26.773	4.438×10^{-6}
Seed 0.95	-33.714	8.997	8.928	26.773	4.438×10^{-6}

Table 24: SLL , $HPBW_{az}$, $HPBW_{el}$, D , Mask Fitting of Radiation Pattern along $(\theta_0, \phi_0) = (0, 0)$ [deg]

Conclusion

The best solution with OTM-GA corresponds to the solution with the best average performance between all the solutions generated, “best” means the solution with minimum average fitness value. In this test case the best solution corresponds to OTM-GA integer with population generated with Hidden Markov Model with the following features:

- Number of individuals - $N_I = 542$
- Number of flips - $N_{flips} = 1 \times 10^5$

1.3 OTM - Binary vs. Integer - Hexagon (10,10,10) - Mask Matching - Steering

$$(\theta, \phi) = (30, 0) [deg] - d_{y2} = 0.5\lambda$$

Array Geometry

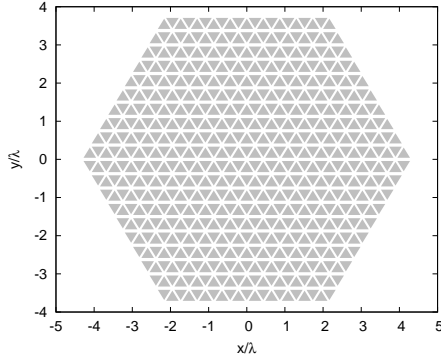


Figure 19: $N_{tot} = 600$, $L_d = 20\lambda$, $d_x = 0.22\lambda$, $d_{y1} = 0.25\lambda$, $d_{y2} = 0.5\lambda$, $N_c^{tot} = 800$, $N_p^{tot} = 441$, $N_p^{(bound)} = 61$, $a = 10$, $b = 10$, $c = 10$ – Array Geometry

Reference Array, Convex Programming Excitations

Test case parameters

- Number of array elements - $N_{tot} = 600$
- Element spacing along x - $d_x = 0.22\lambda$
- Element spacing along y_1 - $d_{y1} = 0.25\lambda$
- Element spacing along y_2 - $d_{y2} = 0.5\lambda$
- Pointing Direction - $\theta_0 = 30^\circ$
- Pointing Direction - $\phi_0 = 0^\circ$
- Pointing Direction - $u_0 = 0.5$
- Pointing Direction - $v_0 = 0$
- A side length - $a = 10$
- B side length - $b = 10$
- C side length - $c = 10$

Mask Constraints

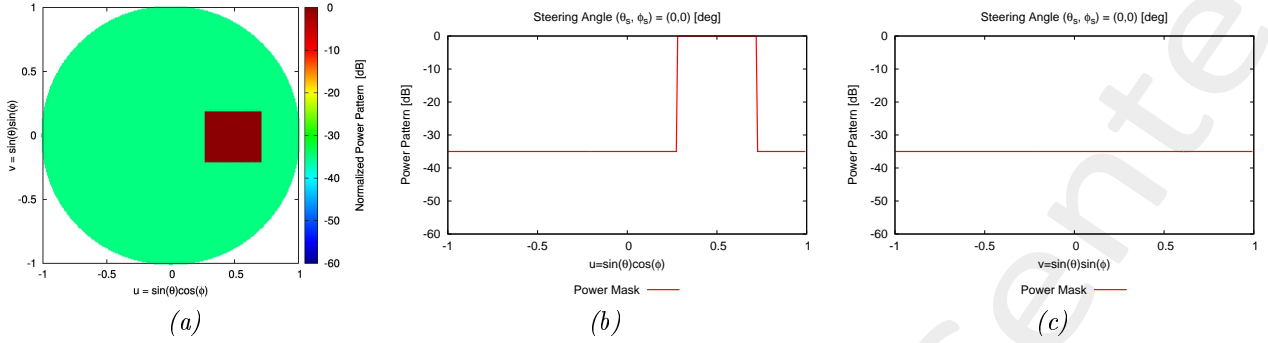


Figure 20: Mask Power Pattern in broadside direction $(\theta, \phi) = (30, 0)$ [deg]: (a) 2D, (b) Normalized cut along azimuth direction, (c) Normalized cut along elevation direction.

Array Tiling

Software Parameters

- Number of array elements - $N_{tot} = 600$
- Element spacing along x - $d_x = 0.22\lambda$
- Element spacing along y_1 - $d_{y1} = 0.25\lambda$
- Element spacing along y_2 - $d_{y2} = 0.5\lambda$
- Side's domain - $L_d = 20\lambda$
- Points number - $N_p^{tot} = 441$
- Points along x - $M_p = 21$
- Points along y - $N_p = 21$
- Total cells number - $N_c^{tot} = 800$
- Cells along x - $M_c = 40$
- Cells along y - $N_c = 20$
- Boundary points - $N_p^{(bound)} = 61$
- Samples along u - $N_u = 256$
- Samples along v - $N_v = 256$
- SLL weight - $w_{SLL} = 0.0$
- Directivity weight - $w_D = 0$

- HPBW weight azimuth - $w_{HPBW}^{azm} = 0.0$
- HPBW weight elevation - $w_{HPBW}^{elv} = 0.0$
- Mask weight - $w_{mask} = 1.0$
- Cell elements - $N_{el} = 1$
- Pointing Direction - $\theta_0 = 30^\circ$
- Pointing Direction - $\phi_0 = 0^\circ$
- Pointing Direction - $u_0 = 0.5$
- Pointing Direction - $v_0 = 0$
- A side length - $a = 10$
- B side length - $b = 10$
- C side length - $c = 10$
- A side length in λ - $L_a = 4.33\lambda$
- B side length in λ - $L_b = 4.33\lambda$
- C side length in λ - $L_c = 4.33\lambda$
- Tiling configurations - $T = 9.27 \times 10^{33}$
- Number of unknowns - $N_u = 1084$
- Maximum of word max - $U_{max} = 10$
- Number of trials (seed) - $N_{seed} = 99$
- Cross-Over probability - $p_{cx} = 0.9$
- Mutation probability - $p_m = 0.001$

Results

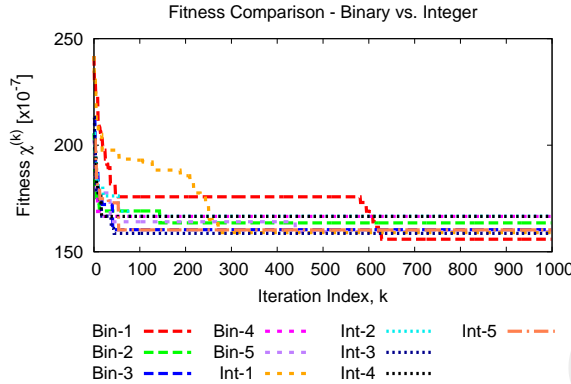


Figure 21: Best 10 fitness for binary and integer coding for the same initial population

The meaning of labels in Fig.21 is stated in Tab.11.

Label	Minimum	Maximum	Average	Variance
<i>Bin</i> – 1	1.559×10^{-5}	2.047×10^{-5}	1.833×10^{-5}	2.367×10^{-12}
<i>Bin</i> – 2	1.636×10^{-5}	1.809×10^{-5}	1.684×10^{-5}	4.976×10^{-14}
<i>Bin</i> – 3	1.604×10^{-5}	1.807×10^{-5}	1.687×10^{-5}	2.445×10^{-13}
<i>Bin</i> – 4	1.666×10^{-5}	1.866×10^{-5}	1.762×10^{-5}	3.198×10^{-13}
<i>Bin</i> – 5	1.594×10^{-5}	1.808×10^{-5}	1.705×10^{-5}	2.480×10^{-13}
<i>Int</i> – 1	1.589×10^{-5}	2.047×10^{-5}	1.934×10^{-5}	1.476×10^{-12}
<i>Int</i> – 2	1.667×10^{-5}	1.816×10^{-5}	1.691×10^{-5}	4.775×10^{-14}
<i>Int</i> – 3	1.587×10^{-5}	1.809×10^{-5}	1.731×10^{-5}	3.261×10^{-13}
<i>Int</i> – 4	1.666×10^{-5}	1.832×10^{-5}	1.751×10^{-5}	4.669×10^{-13}
<i>Int</i> – 5	1.603×10^{-5}	1.808×10^{-5}	1.696×10^{-5}	3.680×10^{-13}

Table 27: Statistics of all fitness in Fig.22

Fig. 21 represents the best fitness value for binary and integer case for 5 different initial populations.

I analyzed the solution that permits to reach the minimum fitness value, associated with the minimum average value. The fitness to analize is *Bin* – 2.

The parameters for this test case are:

- Number of individuals - $N_I = 272$
- Number of flips - $N_{flips} = 200$
- Coding Type - Binary

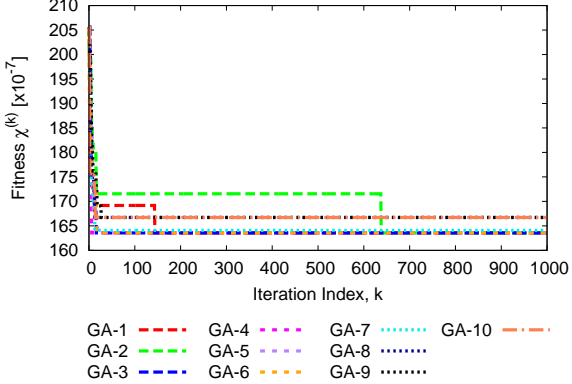


Figure 22: Fitness for 10 best seeds

GA	Seed	SLL [dB]	HPBW (az) [deg]	HPBW (el) [deg]	D [dB]	Fitness Value
1	0.199	-33.675	8.996	8.928	26.773	1.636×10^{-5}
2	0.551	-33.675	8.996	8.928	26.773	1.636×10^{-5}
3	0.559	-33.675	8.996	8.928	26.773	1.636×10^{-5}
4	0.682	-33.675	8.996	8.928	26.773	1.636×10^{-5}
5	0.846	-33.675	8.996	8.928	26.773	1.636×10^{-5}
6	0.9	-33.675	8.996	8.928	26.773	1.636×10^{-5}
7	0.75	-33.674	8.996	8.928	26.774	1.641×10^{-5}
8	0.05	-33.739	8.997	8.929	26.773	1.667×10^{-5}
9	0.067	-33.739	8.997	8.929	26.773	1.667×10^{-5}
10	0.087	-33.739	8.997	8.929	26.773	1.667×10^{-5}

Table 29: Solution Parameters of Radiation Pattern along $(\theta_0, \phi_0) = (0, 0)$ [deg]

Fig.22 rappresents the fitness value for 10 best seeds.

I analyzed the solution (seed) that permits to reach the minimum fitness value. The solutions analized corresponds to *seed* = {0.199}.

Broadside Analysis

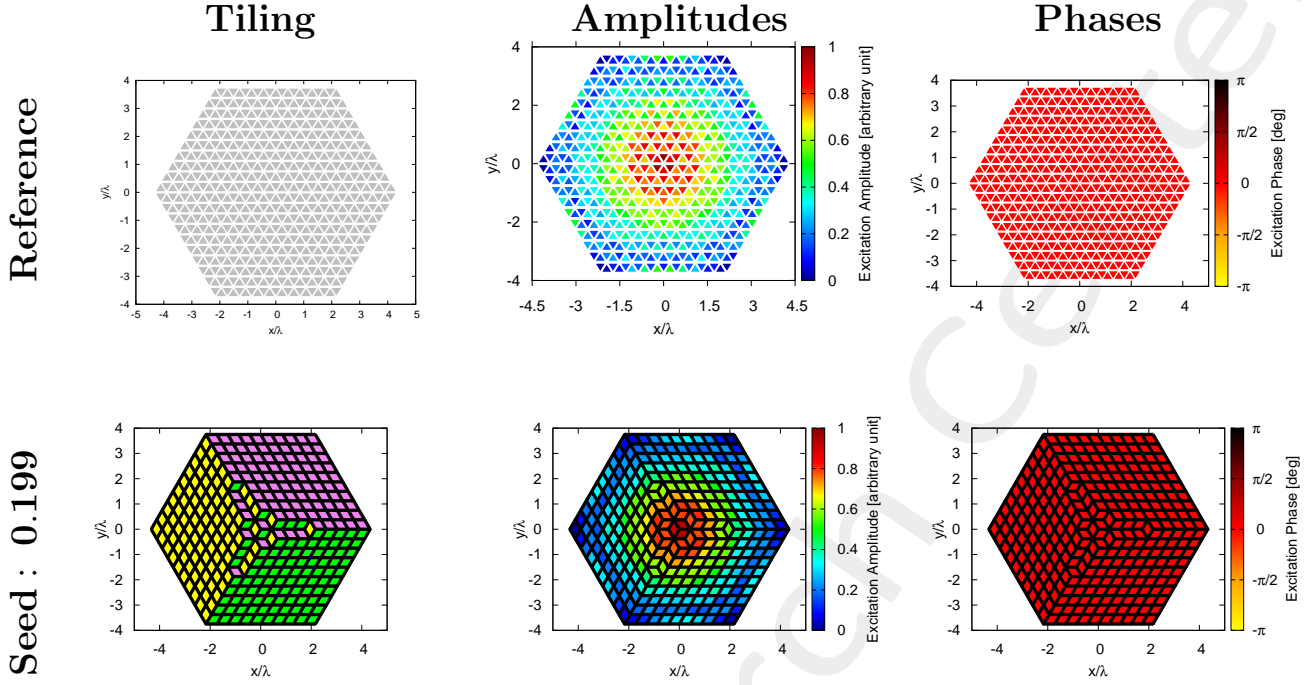


Figure 23: *Mask Matching*, $SLL = -34.79$ [dB], $N_{tot} = 600$, $L_d = 20\lambda$, $d_x = 0.22\lambda$, $d_{y1} = 0.25\lambda$, $d_{y2} = 0.5\lambda$, $a = 10$, $b = 10$, $c = 10$, $(\theta_0, \phi_0) = (0, 0)$ [deg] – Solution ID.: Reference, Seed 0.199

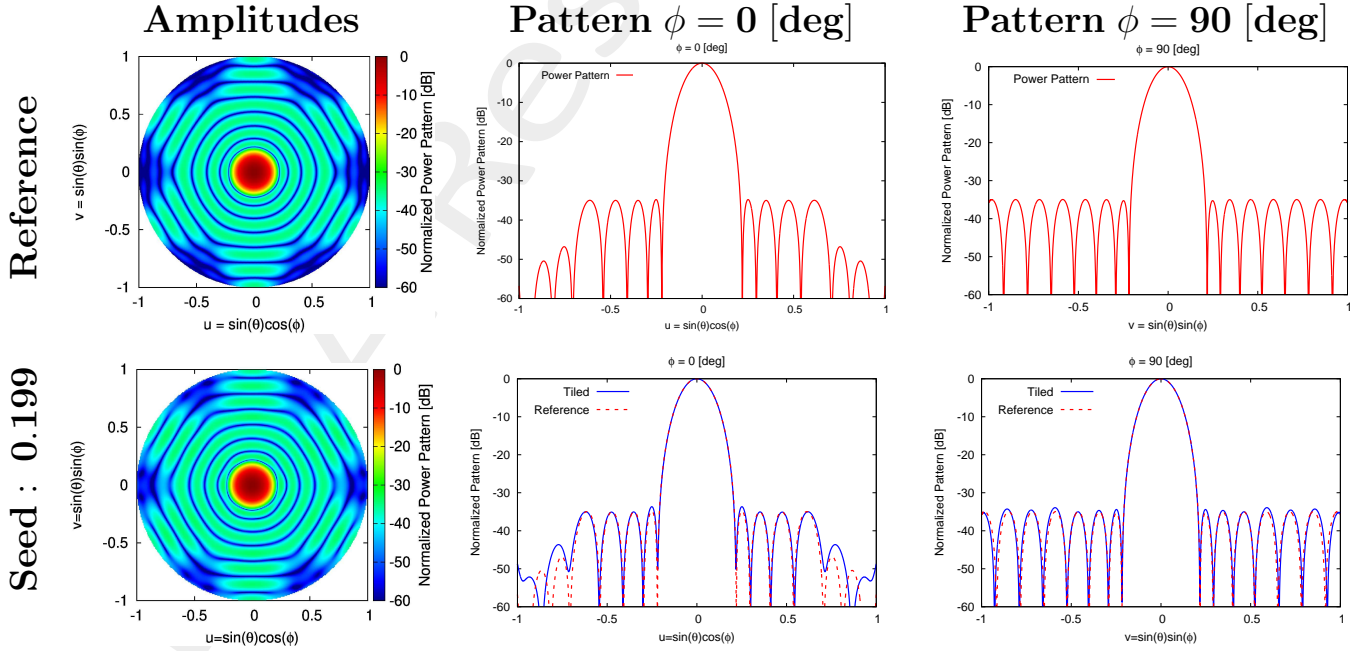


Figure 24: *Mask Matching*, $SLL = -34.79$ [dB], $N_{tot} = 600$, $L_d = 20\lambda$, $d_x = 0.22\lambda$, $d_{y1} = 0.25\lambda$, $d_{y2} = 0.5\lambda$, $a = 10$, $b = 10$, $c = 10$, $(\theta_0, \phi_0) = (0, 0)$ [deg] – Solution ID.: Reference, Seed 0.199

Steering Analysis

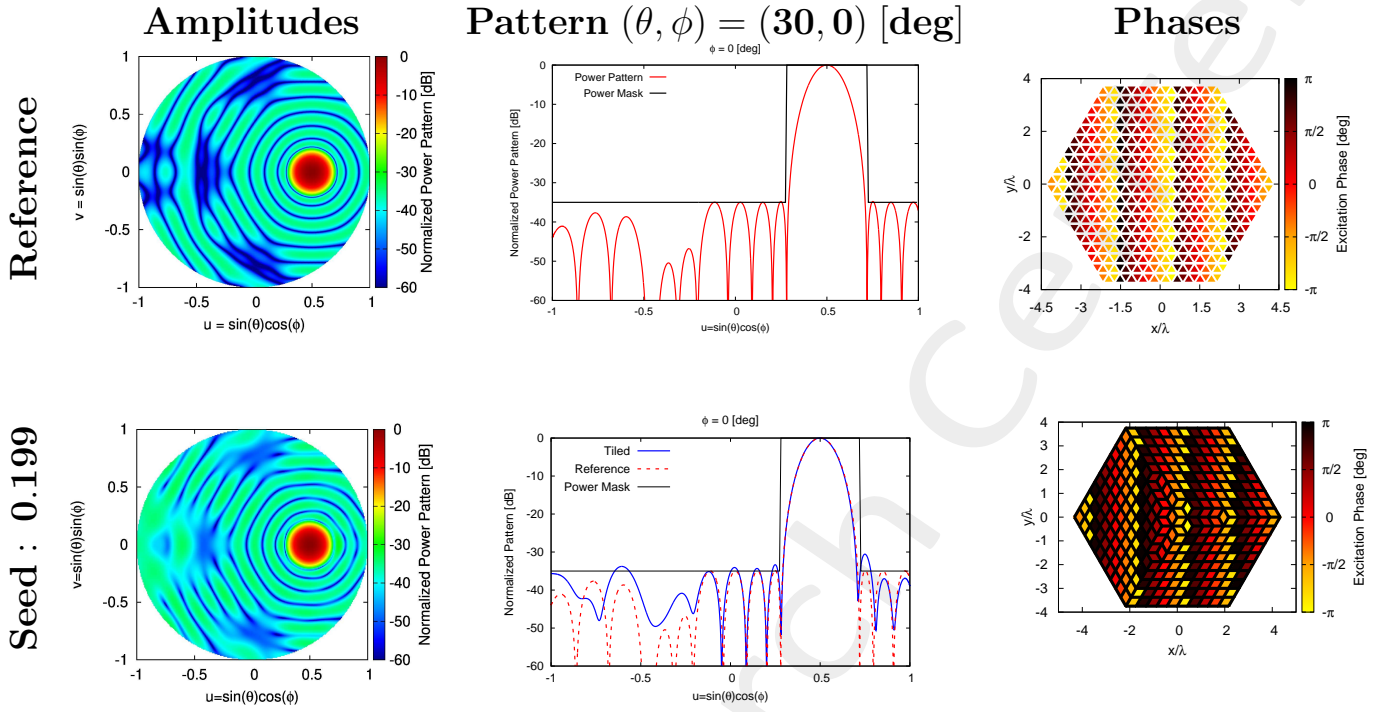


Figure 25: *Mask Matching*, $SLL = -34.79$ [dB], $N_{tot} = 600$, $L_d = 20\lambda$, $d_x = 0.22\lambda$, $d_{y1} = 0.25\lambda$, $d_{y2} = 0.5\lambda$, $a = 10$, $b = 10$, $c = 10$, $(\theta_0, \phi_0) = (30, 0)$ [deg] – Solution ID.: Reference, Seed 0.199

Solutions Summary

(a, b, c)	MAX_ITE (# iterations)	$\Delta\tau$ [sec] (single simulation period)	τ [sec] total simulation period
10, 10, 10	1000	0.173497	173.497

Table 33: Simulation Time

SOLUTION ID	SLL [dB]	HPBW (azimuth) [deg]	HPBW (elevation) [deg]	D [dB]	Mask Fitting
Reference	-34.788	9.003	8.914	26.791	0
Seed 0.199	-33.675	8.996	8.928	26.773	1.636×10^{-5}

Table 34: SLL , $HPBW_{az}$, $HPBW_{el}$, D , Mask Fitting of Radiation Pattern along $(\theta_0, \phi_0) = (0, 0)$ [deg]

Conclusion

The best solution with OTM-GA corresponds to the solution with the best average performance between all the solutions generated, “best” means the solution with minimum average fitness value. In this test case the best solution corresponds to OTM-GA binary with population generated with Hidden Markov Model with the following features:

- Number of individuals - $N_I = 272$
- Number of flips - $N_{flips} = 200$

1.4 OTM - Integer - Hexagon (10,10,10) - Mask Matching - Broadside - $d_{y2} = 0.69\lambda$

Array Geometry

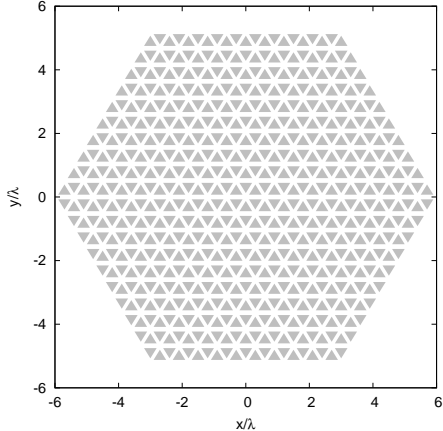


Figure 26: $N_{tot} = 600$, $L_d = 20\lambda$, $d_x = 0.3\lambda$, $d_{y1} = 0.35\lambda$, $d_{y2} = 0.69\lambda$, $N_c^{tot} = 800$, $N_p^{tot} = 441$, $N_p^{(bound)} = 61$, $a = 10$, $b = 10$, $c = 10$ – Array Geometry

Reference Array, Convex Programming Excitations

Test case parameters

- Number of array elements - $N_{tot} = 600$
- Element spacing along x - $d_x = 0.3\lambda$
- Element spacing along y_1 - $d_{y1} = 0.35\lambda$
- Element spacing along y_2 - $d_{y2} = 0.69\lambda$
- Pointing Direction - $\theta_0 = 0^\circ$
- Pointing Direction - $\phi_0 = 0^\circ$
- Pointing Direction - $u_0 = 0$
- Pointing Direction - $v_0 = 0$
- A side length - $a = 10$
- B side length - $b = 10$
- C side length - $c = 10$

Mask Constraints

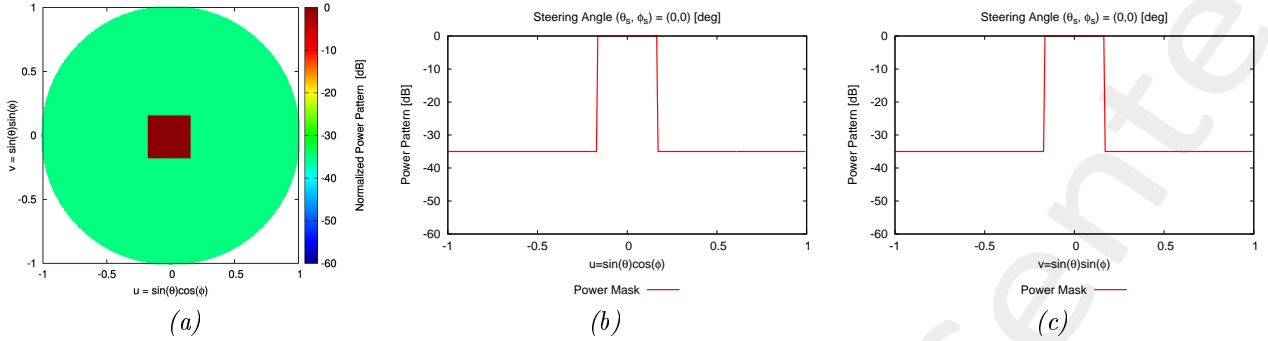


Figure 27: Mask Power Pattern in broadside direction $(\theta, \phi) = (0, 0)$ [deg]: (a) 2D, (b) Normalized cut along azimuth direction, (c) Normalized cut along elevation direction.

Array Tiling

Software Parameters

- Number of array elements - $N_{tot} = 600$
- Element spacing along x - $d_x = 0.3\lambda$
- Element spacing along y_1 - $d_{y1} = 0.35\lambda$
- Element spacing along y_2 - $d_{y2} = 0.69\lambda$
- Side's domain - $L_d = 20\lambda$
- Points number - $N_p^{tot} = 441$
- Points along x - $M_p = 21$
- Points along y - $N_p = 21$
- Total cells number - $N_c^{tot} = 800$
- Cells along x - $M_c = 40$
- Cells along y - $N_c = 20$
- Boundary points - $N_p^{(bound)} = 61$
- Samples along u - $N_u = 256$
- Samples along v - $N_v = 256$
- SLL weight - $w_{SLL} = 0.0$
- Directivity weight - $w_D = 0$

- HPBW weight azimuth - $w_{HPBW}^{azm} = 0.0$
- HPBW weight elevation - $w_{HPBW}^{elv} = 0.0$
- Mask weight - $w_{mask} = 1.0$
- Cell elements - $N_{el} = 1$
- Pointing Direction - $\theta_0 = 0^\circ$
- Pointing Direction - $\phi_0 = 0^\circ$
- Pointing Direction - $u_0 = 0$
- Pointing Direction - $v_0 = 0$
- A side length - $a = 10$
- B side length - $b = 10$
- C side length - $c = 10$
- A side length in λ - $L_a = 6\lambda$
- B side length in λ - $L_b = 6\lambda$
- C side length in λ - $L_c = 6\lambda$
- Tiling configurations - $T = 9.27 \times 10^{33}$
- Number of unknowns - $N_u = 1084$
- Maximum of word max - $U_{max} = 10$
- Number of trials (seed) - $N_{seed} = 103$
- Cross-Over probability - $p_{cx} = 0.9$
- Mutation probability - $p_m = 0.001$

Results

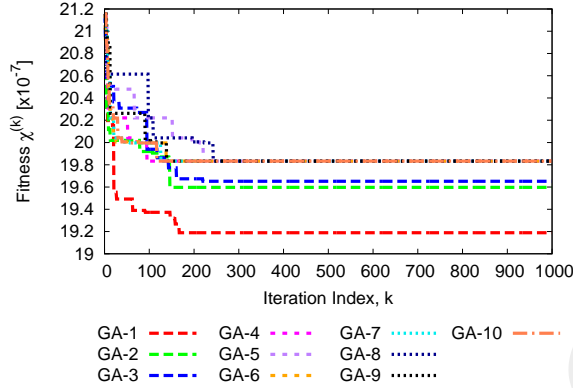


Figure 28: Fitness for 10 best seeds

GA	Seed	SLL [dB]	HPBW (az) [deg]	HPBW (el) [deg]	D [dB]	Fitness Value
1	0.05	-32.968	6.429	6.544	29.619	1.919×10^{-6}
2	0.9	-32.869	6.426	6.544	29.622	1.959×10^{-6}
3	0.8	-32.879	6.426	6.544	29.622	1.965×10^{-6}
4	0.087	-32.902	6.428	6.544	29.621	1.983×10^{-6}
5	0.441	-32.902	6.428	6.544	29.621	1.983×10^{-6}
6	0.445	-32.902	6.428	6.544	29.621	1.983×10^{-6}
7	0.469	-32.902	6.428	6.544	29.621	1.983×10^{-6}
8	0.484	-32.902	6.428	6.544	29.621	1.983×10^{-6}
9	0.4	-32.902	6.428	6.544	29.621	1.983×10^{-6}
10	0.5	-32.902	6.428	6.544	29.621	1.983×10^{-6}

Table 37: Solution Parameters of Radiation Pattern along $(\theta_0, \phi_0) = (0, 0)$ [deg]

Fig.28 rappresents the fitness value for 10 best seeds.

I analyzed the solution (seed) that permits to reach the minimum fitness value. The solutions analized corresponds to $seed = \{0.05\}$.

Best Individuals

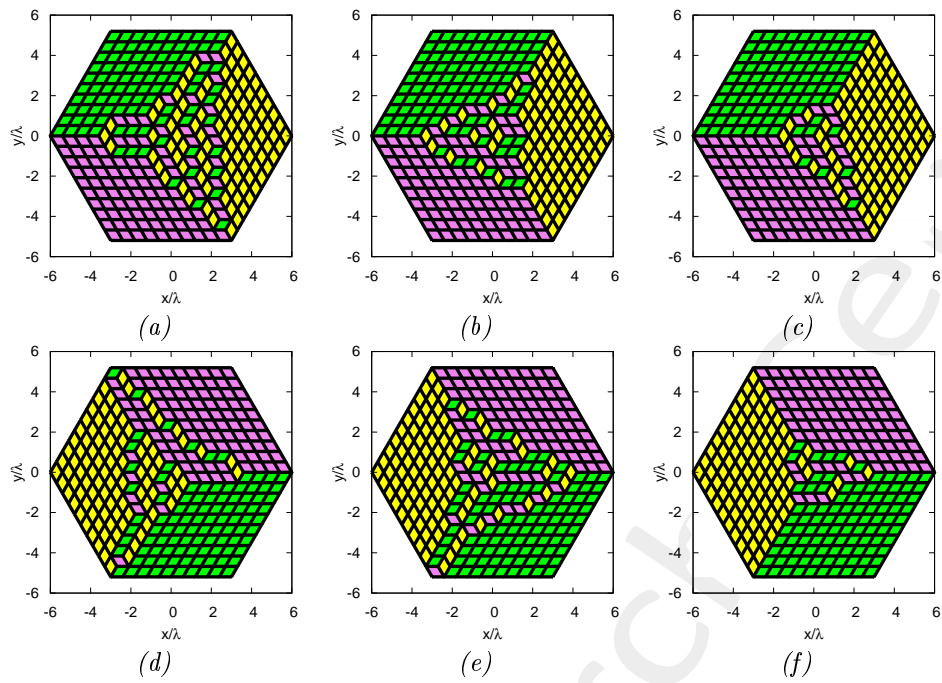


Figure 29: Best individuals of initial population: (a) Individual nr. 55, (b) Individual nr. 64, (c) Individual nr. 86, (d) Individual nr. 105, (e) Individual nr. 223, (f) Individual nr. 241.

Broadside Analysis

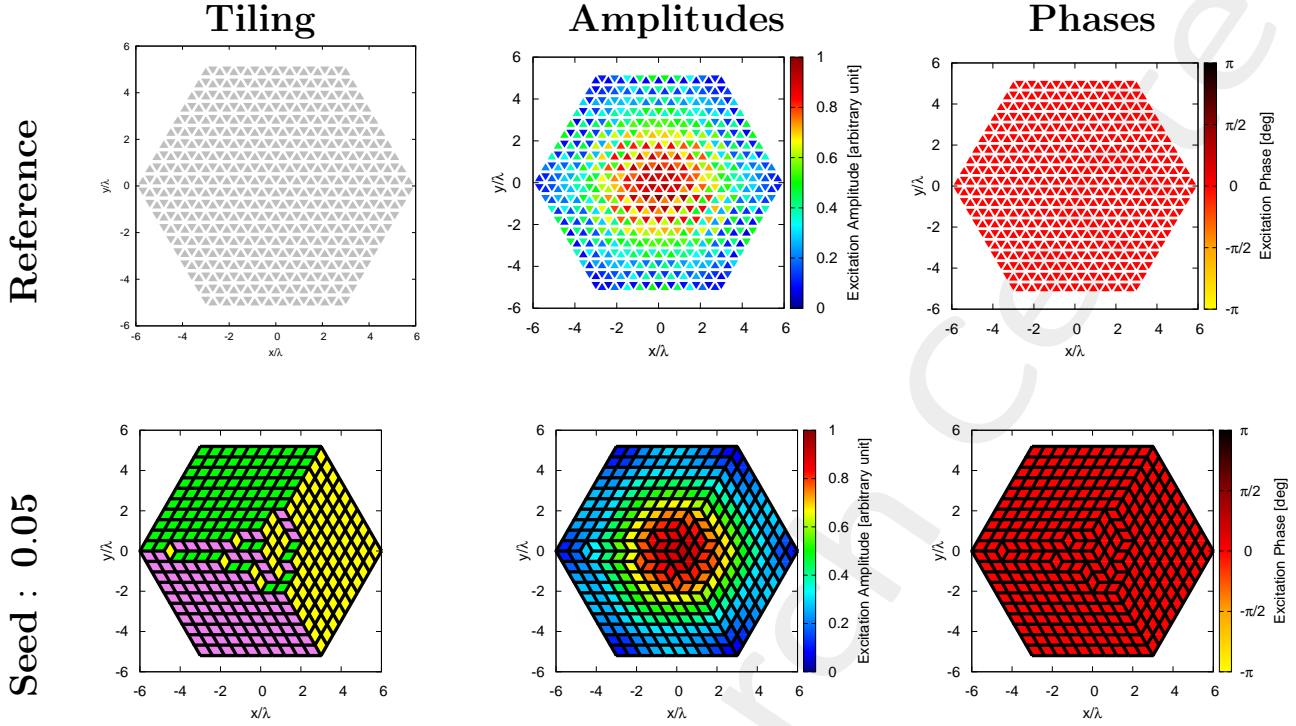


Figure 30: *Mask Matching*, $SLL = -34.31$ [dB], $N_{tot} = 600$, $L_d = 20\lambda$, $d_x = 0.3\lambda$, $d_{y1} = 0.35\lambda$, $d_{y2} = 0.69\lambda$, $a = 10$, $b = 10$, $c = 10$, $(\theta_0, \phi_0) = (0, 0)$ [deg] – Solution ID.: Reference, Seed 0.514

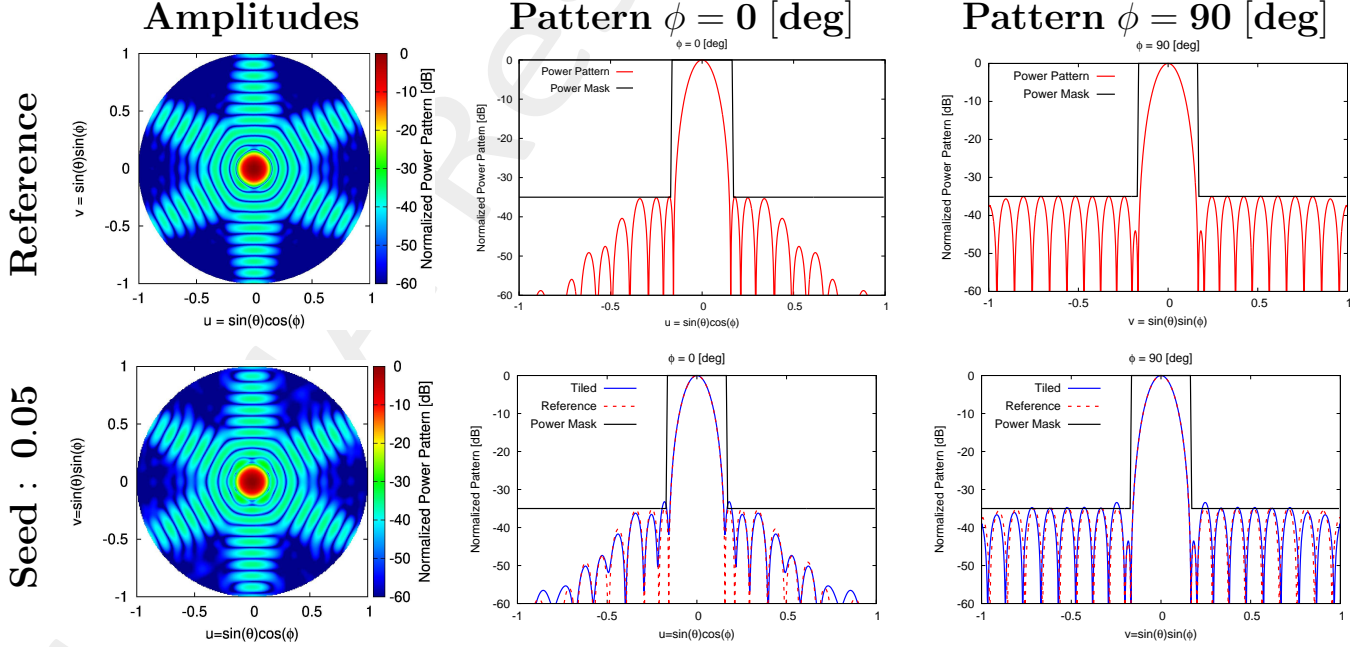


Figure 31: *Mask Matching*, $SLL = -34.31$ [dB], $N_{tot} = 600$, $L_d = 20\lambda$, $d_x = 0.3\lambda$, $d_{y1} = 0.35\lambda$, $d_{y2} = 0.69\lambda$, $a = 10$, $b = 10$, $c = 10$, $(\theta_0, \phi_0) = (0, 0)$ [deg] – Solution ID.: Reference, Seed 0.05

Steering Analysis

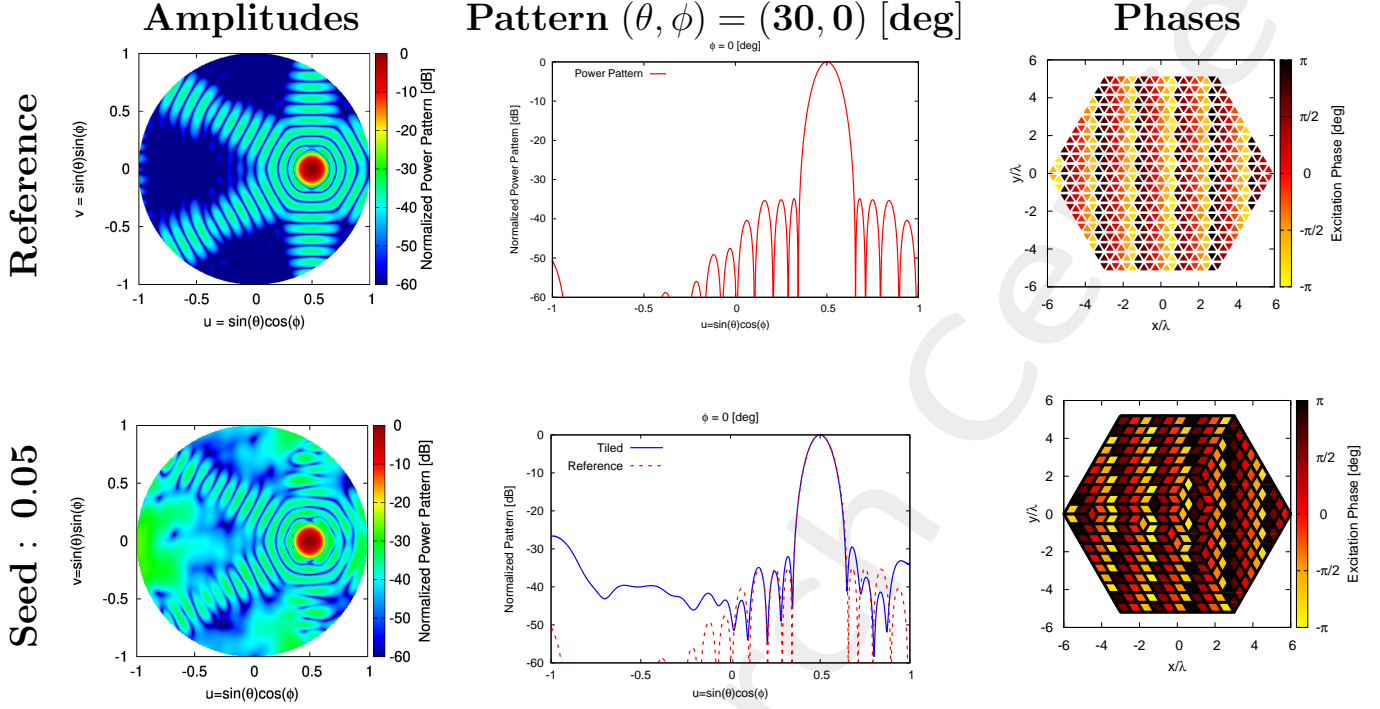


Figure 32: *Mask Matching*, $SLL = -34.31$ [dB], $N_{tot} = 600$, $L_d = 20\lambda$, $d_x = 0.3\lambda$, $d_{y1} = 0.35\lambda$, $d_{y2} = 0.69\lambda$, $a = 10$, $b = 10$, $c = 10$, $(\theta_0, \phi_0) = (30, 0)$ [deg] – Solution ID.: Reference, Seed 0.05

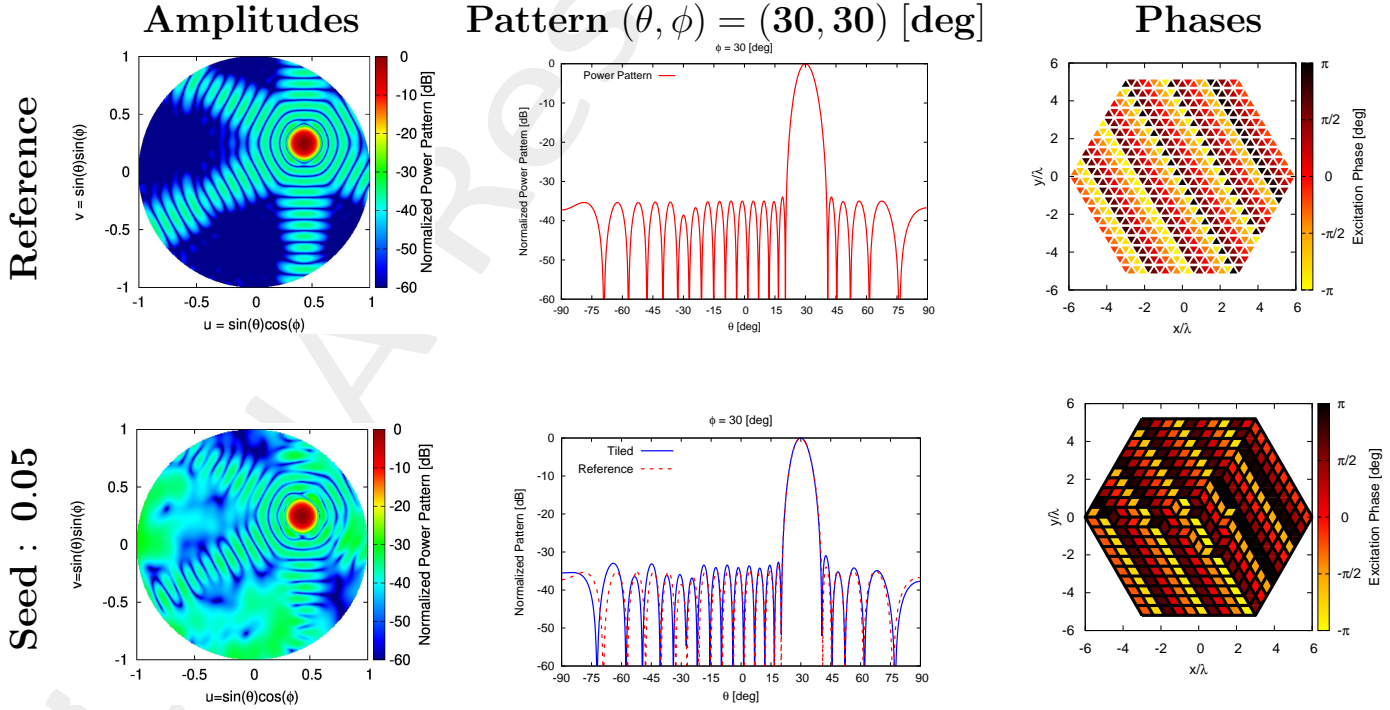


Figure 33: *Mask Matching*, $SLL = -34.31$ [dB], $N_{tot} = 600$, $L_d = 20\lambda$, $d_x = 0.3\lambda$, $d_{y1} = 0.35\lambda$, $d_{y2} = 0.69\lambda$, $a = 10$, $b = 10$, $c = 10$, $(\theta_0, \phi_0) = (30, 30)$ [deg] – Solution ID.: Reference, Seed 0.05

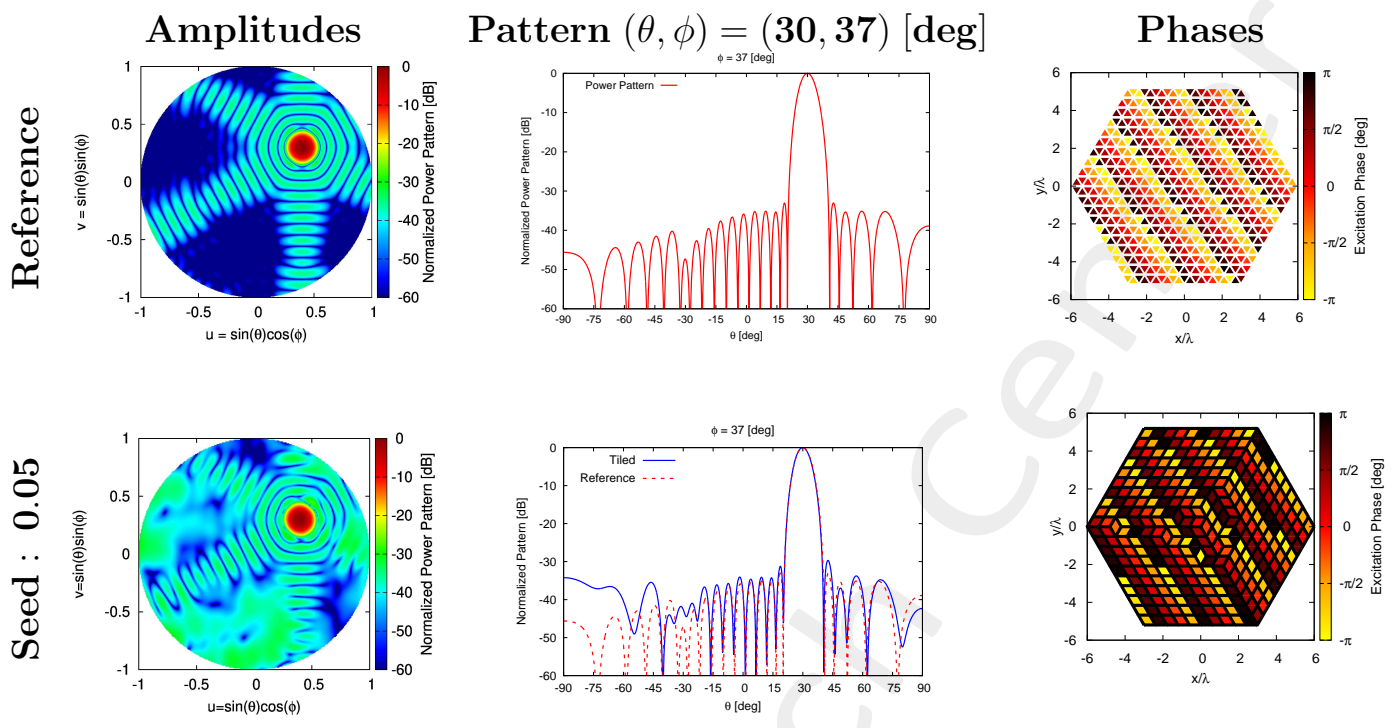


Figure 34: *Mask Matching*, $SLL = -34.31$ [dB], $N_{tot} = 600$, $L_d = 20\lambda$, $d_x = 0.3\lambda$, $d_{y1} = 0.35\lambda$, $d_{y2} = 0.69\lambda$, $a = 10$, $b = 10$, $c = 10$, $(\theta_0, \phi_0) = (30, 37)$ [deg] – Solution ID.: Reference, Seed 0.05

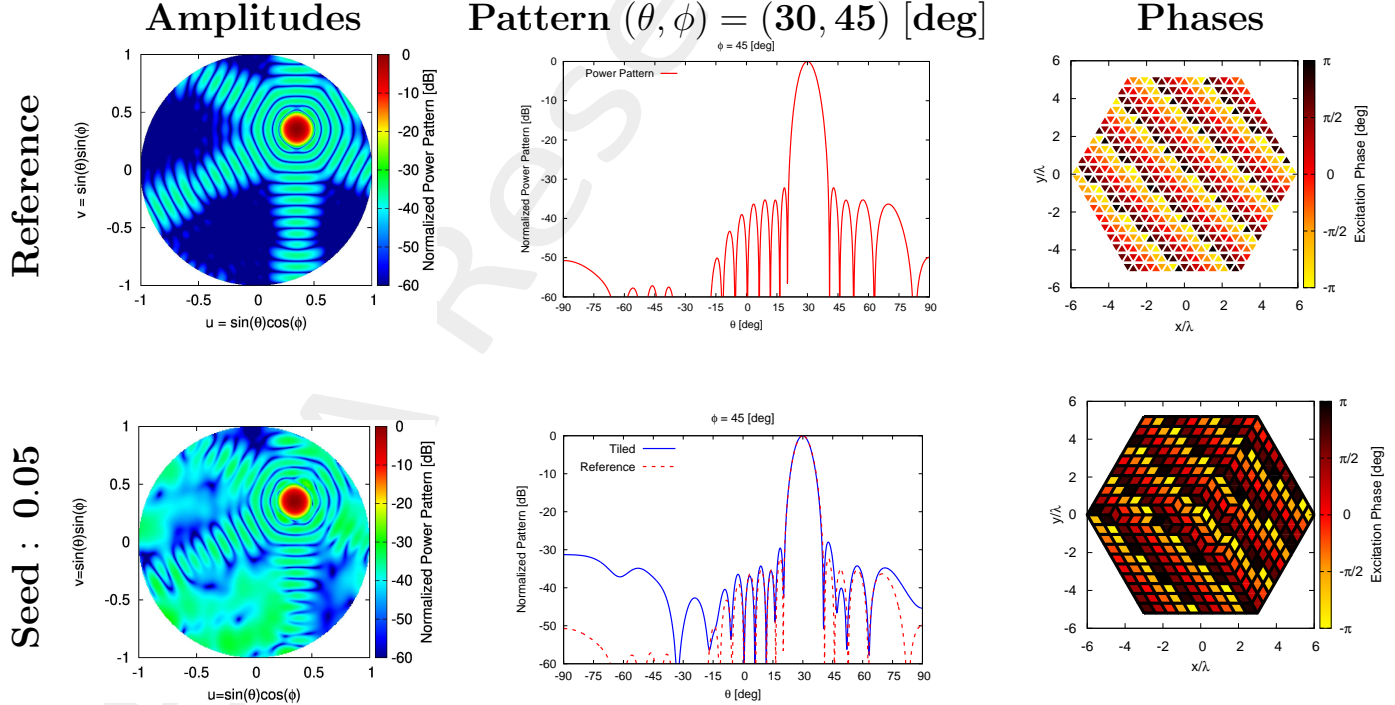


Figure 35: *Mask Matching*, $SLL = -34.31$ [dB], $N_{tot} = 600$, $L_d = 20\lambda$, $d_x = 0.3\lambda$, $d_{y1} = 0.35\lambda$, $d_{y2} = 0.69\lambda$, $a = 10$, $b = 10$, $c = 10$, $(\theta_0, \phi_0) = (30, 45)$ [deg] – Solution ID.: Reference, Seed 0.05

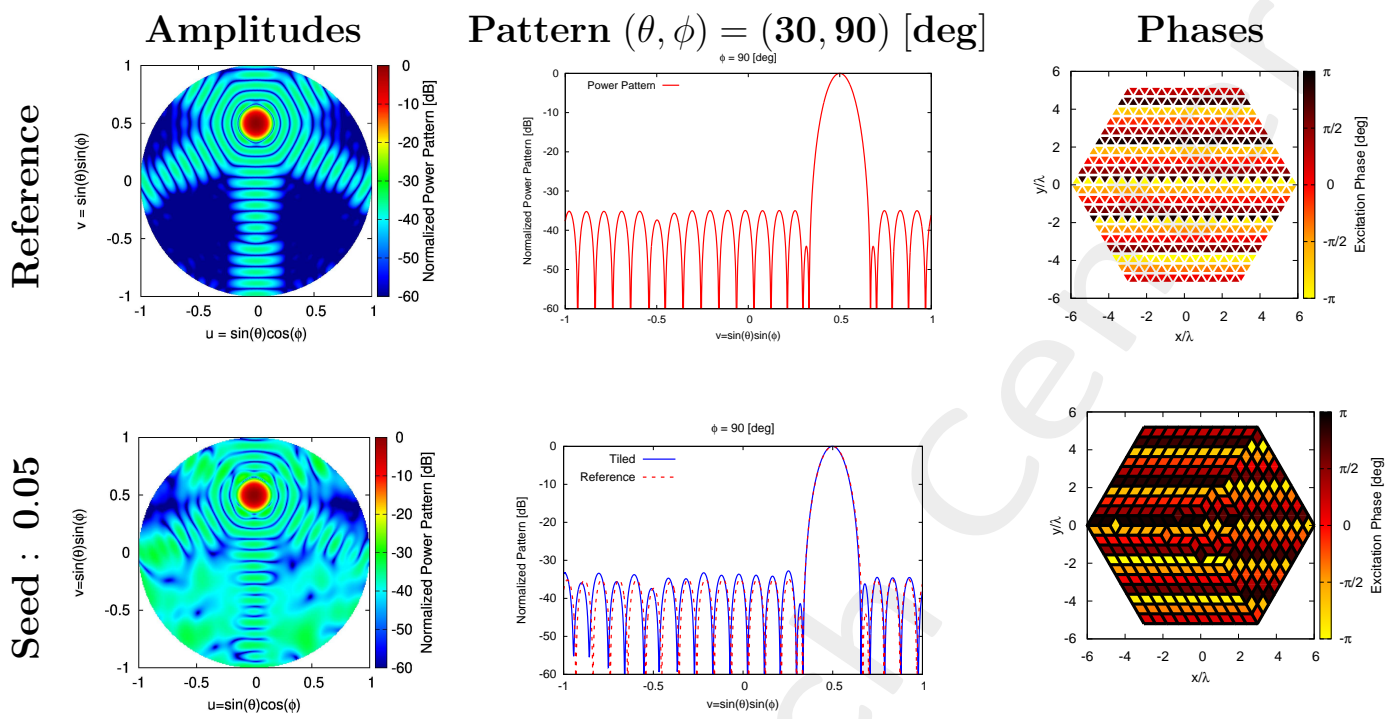


Figure 36: *Mask Matching*, $SLL = -34.31$ [dB], $N_{tot} = 600$, $L_d = 20\lambda$, $d_x = 0.3\lambda$, $d_{y1} = 0.35\lambda$, $d_{y2} = 0.69\lambda$, $a = 10$, $b = 10$, $c = 10$, $(\theta_0, \phi_0) = (30, 90)$ [deg] – Solution ID.: Reference, Seed 0.05

Solutions Summary

(a, b, c)	MAX_ITE (# iterations)	$\Delta\tau$ [sec] (single simulation period)	τ [sec] total simulation period
10, 10, 10	1000	0.047321	47.321

Table 46: Simulation Time

SOLUTION ID	SLL [dB]	HPBW (azimuth) [deg]	HPBW (elevation) [deg]	D [dB]	Mask Fitting
Reference	-34.305	6.392	6.515	29.653	0
Seed 0.05	-32.968	6.429	6.544	29.619	1.919×10^{-6}

Table 47: SLL , $HPBW_{az}$, $HPBW_{el}$, D , Mask Fitting of Radiation Pattern along $(\theta_0, \phi_0) = (0, 0)$ [deg]

Conclusion

The solution with OTM-GA [Sec.1.4] is a good choice respect to ETM for the same array architecture; because it is possible to obtain good results with less computational effort.

2 Conclusions

An innovative approach for the design of hexagonal aperture phased arrays clustered with diamond shaped tile in three different orientation: vertical σ^V , horizontal-left $\sigma^{H_{left}}$ and horizontal-right $\sigma^{H_{right}}$ has been implemented and validated.

The first strategy is called Enumerative Tiling Method (ETM), it has been developed for low/medium size aperture and it permits to retrieve the globally-optimal solution by exploring the entire solution spaces by using mathematical theorems and algorithms.

The second one is called Optimization Tiling Method (OTM), it has been developed for large arrays size, it is a GA-based optimization strategy and it has been proposed with two different implementations: binary (OTM-BGA) and integer-coding (OTM-IGA).

The main advantages of there approaches are:

- ETM permits to retrieve the globally-optimal solution of solution space with low cardinality, thanks to mathematical theorems and algorithms, therefore the best tiling configuration is that associated with minimum mask matching value, it is the one more close to reference solution;
- OTM permits to tile large aperture, therefore solution space with high cardinality, by exploring a subset of solutions space by an analytic definition of initial tiling configurations and a GA-based approach. The novelty is the integer coding, that permits to reduce the computational effort and to converge to a best or equal solution of binary coding at SoA

To valide this approach a more detailed analysis has been considered:

- an exploration of the whole solution space is done with exhaustive method (ETM), but ETM shows that only a sub-set of solutions is close to reference architecture, therefore is possible to analyze a subset of solutions to retrieve one of the best tiling configuration, to do this GA algorithms are robust because for small/medium aperture permits to find the globally-optimal solution, the use of GAs become necessary for high cardinality solution space, so for large arrays;
- on the actual SoA literature, GAs are implemented using binary coding (OTM-BGA), this strategy permits to converge to a solution close to reference case, so GAs are a robust solution, but if array aperture become large, the binary string become long, so the computational time increase;
- to reduce the string lenght the new method proposed uses integer coding, so each tiling configuration is coded with a series of integer numbers (OTM-IGA), short string means low computational time and the convergence value is close or best than OTM-BGA case;
- considering real radiating elements, performance are closed to ideal/isotropic case;
- compared the solution of SoA with the approach proposed, for both cases the solutions are close to reference one, but the new method recude computational time;

- the solutions list of ETM and OTM are non-unique value, so this permits to array designer to select a configuration that fits addition requirements;
- ETM and OTM are good solutions to synthesize array architecture for broadside direction $(\theta_0, \phi_0) = (0, 0)$ [deg] and a required steering direction (θ_0, ϕ_0) .

For future research activities, this new methodology will be extended ETM and OTM:

- for tiling hexagonal aperture with regular and irregular shape, by using poly-iamond, therefore tiles composed by more than 2 equilateral triangles, in order to reduce further the number of control points;
- reduce the solution space by exploiting simmetries on the solution set, in order to have more probability to find the optimal solution also for GAs;
- implements GAs with hexadecimal coding, in order to increase further the array dimension and to reduce computational effort.

More information on the topics of this document can be found in the following list of references.

References

- [1] P. Rocca, M. Benedetti, M. Donelli, D. Franceschini, and A. Massa, "Evolutionary optimization as applied to inverse problems," *Inverse Problems - 25 th Year Special Issue of Inverse Problems, Invited Topical Review*, vol. 25, pp. 1-41, Dec. 2009
- [2] P. Rocca, G. Oliveri, and A. Massa, "Differential Evolution as applied to electromagnetics," *IEEE Antennas Propag. Mag.*, vol. 53, no. 1, pp. 38-49, Feb. 2011
- [3] P. Rocca, N. Anselmi, A. Polo, and A. Massa, "An irregular two-sizes square tiling method for the design of isophoric phased arrays," *IEEE Trans. Antennas Propag.*, vol. 68, no. 6, pp. 4437-4449, Jun. 2020
- [4] P. Rocca, N. Anselmi, A. Polo, and A. Massa, "Modular design of hexagonal phased arrays through diamond tiles," *IEEE Trans. Antennas Propag.*, vol. 68, no. 5, pp. 3598-3612, May 2020
- [5] N. Anselmi, L. Poli, P. Rocca, and A. Massa, "Design of simplified array layouts for preliminary experimental testing and validation of large AESAs," *IEEE Trans. Antennas Propag.*, vol. 66, no. 12, pp. 6906-6920, Dec. 2018
- [6] N. Anselmi, P. Rocca, M. Salucci, and A. Massa, "Contiguous phase-clustering in multibeam-on-receive scanning arrays," *IEEE Trans. Antennas Propag.*, vol. 66, no. 11, pp. 5879-5891, Nov. 2018
- [7] G. Oliveri, G. Gottardi, F. Robol, A. Polo, L. Poli, M. Salucci, M. Chuan, C. Massagrande, P. Vinetti, M. Mattivi, R. Lombardi, and A. Massa, "Co-design of unconventional array architectures and antenna elements for 5G base station," *IEEE Trans. Antennas Propag.*, vol. 65, no. 12, pp. 6752-6767, Dec. 2017
- [8] N. Anselmi, P. Rocca, M. Salucci, and A. Massa, "Irregular phased array tiling by means of analytic schemata-driven optimization," *IEEE Trans. Antennas Propag.*, vol. 65, no. 9, pp. 4495-4510, September 2017
- [9] N. Anselmi, P. Rocca, M. Salucci, and A. Massa, "Optimization of excitation tolerances for robust beam-forming in linear arrays," *IET Microwaves, Antennas & Propagation*, vol. 10, no. 2, pp. 208-214, 2016
- [10] P. Rocca, R. J. Mailloux, and G. Toso, "GA-Based optimization of irregular sub-array layouts for wideband phased arrays desig," *IEEE Antennas and Wireless Propag. Lett.*, vol. 14, pp. 131-134, 2015
- [11] P. Rocca, M. Donelli, G. Oliveri, F. Viani, and A. Massa, "Reconfigurable sum-difference pattern by means of parasitic elements for forward-looking monopulse radar," *IET Radar, Sonar & Navigation*, vol 7, no. 7, pp. 747-754, 2013
- [12] P. Rocca, L. Manica, and A. Massa, "Ant colony based hybrid approach for optimal compromise sum-difference patterns synthesis," *Microwave Opt. Technol. Lett.*, vol. 52, no. 1, pp. 128-132, Jan. 2010

- [13] P. Rocca, L. Manica, and A. Massa, "An improved excitation matching method based on an ant colony optimization for suboptimal-free clustering in sum-difference compromise synthesis," *IEEE Trans. Antennas Propag.*, vol. 57, no. 8, pp. 2297-2306, Aug. 2009
- [14] M. Salucci, L. Poli, A. F. Morabito, and P. Rocca, "Adaptive nulling through subarray switching in planar antenna arrays," *Journal of Electromagnetic Waves and Applications*, vol. 30, no. 3, pp. 404-414, February 2016
- [15] T. Moriyama, L. Poli, and P. Rocca, "Adaptive nulling in thinned planar arrays through genetic algorithms," *IEICE Electronics Express*, vol. 11, no. 21, pp. 1-9, Sep. 2014
- [16] L. Poli, P. Rocca, M. Salucci, and A. Massa, "Reconfigurable thinning for the adaptive control of linear arrays," *IEEE Trans. Antennas Propag.*, vol. 61, no. 10, pp. 5068-5077, Oct. 2013
- [17] P. Rocca, L. Poli, G. Oliveri, and A. Massa, "Adaptive nulling in time-varying scenarios through time-modulated linear arrays," *IEEE Antennas Wireless Propag. Lett.*, vol. 11, pp. 101-104, 2012
- [18] M. Benedetti, G. Oliveri, P. Rocca, and A. Massa, "A fully-adaptive smart antenna prototype: ideal model and experimental validation in complex interference scenarios," *Progress in Electromagnetic Research*, PIER 96, pp. 173-191, 2009
- [19] P. Rocca, L. Poli, A. Polo, and A. Massa, "Optimal excitation matching strategy for sub-arrayed phased linear arrays generating arbitrary shaped beams," *IEEE Trans. Antennas Propag.*, vol. 68, no. 6, pp. 4638-4647, Jun. 2020
- [20] G. Oliveri, G. Gottardi and A. Massa, "A new meta-paradigm for the synthesis of antenna arrays for future wireless communications," *IEEE Trans. Antennas Propag.*, vol. 67, no. 6, pp. 3774-3788, Jun. 2019
- [21] P. Rocca, M. H. Hannan, L. Poli, N. Anselmi, and A. Massa, "Optimal phase-matching strategy for beam scanning of sub-arrayed phased arrays," *IEEE Trans. Antennas and Propag.*, vol. 67, no. 2, pp. 951-959, Feb. 2019
- [22] L. Poli, G. Oliveri, P. Rocca, M. Salucci, and A. Massa, "Long-Distance WPT Unconventional Arrays Synthesis," *Journal of Electromagnetic Waves and Applications*, vol. 31, no. 14, pp. 1399-1420, Jul. 2017
- [23] G. Gottardi, L. Poli, P. Rocca, A. Montanari, A. Aprile, and A. Massa, "Optimal Monopulse Beamforming for Side-Looking Airborne Radars," *IEEE Antennas Wireless Propag. Lett.*, vol. 16, pp. 1221-1224, 2017
- [24] G. Oliveri, M. Salucci, and A. Massa, "Synthesis of modular contiguously clustered linear arrays through a sparseness-regularized solver," *IEEE Trans. Antennas Propag.*, vol. 64, no. 10, pp. 4277-4287, Oct. 2016
- [25] P. Rocca, G. Oliveri, R. J. Mailloux, and A. Massa, "Unconventional phased array architectures and design Methodologies - A review," *Proceedings of the IEEE = Special Issue on 'Phased Array Technologies', Invited Paper*, vol. 104, no. 3, pp. 544-560, March 2016

- [26] P. Rocca, M. D'Urso, and L. Poli, "Advanced strategy for large antenna array design with subarray-only amplitude and phase contr," *IEEE Antennas and Wireless Propag. Lett.*, vol. 13, pp. 91-94, 2014
- [27] L. Manica, P. Rocca, G. Oliveri, and A. Massa, "Synthesis of multi-beam sub-arrayed antennas through an excitation matching strategy," *IEEE Trans. Antennas Propag.*, vol. 59, no. 2, pp. 482-492, Feb. 2011
- [28] G. Oliveri, "Multi-beam antenna arrays with common sub-array layouts," *IEEE Antennas Wireless Propag. Lett.*, vol. 9, pp. 1190-1193, 2010
- [29] P. Rocca, R. Haupt, and A. Massa, "Sidelobe reduction through element phase control in sub-arrayed array antennas," *IEEE Antennas Wireless Propag. Lett.*, vol. 8, pp. 437-440, 2009
- [30] P. Rocca, L. Manica, R. Azaro, and A. Massa, "A hybrid approach for the synthesis of sub-arrayed monopulse linear arrays," *IEEE Trans. Antennas Propag.*, vol. 57, no. 1, pp. 280-283, Jan. 2009
- [31] L. Manica, P. Rocca, M. Benedetti, and A. Massa, "A fast graph-searching algorithm enabling the efficient synthesis of sub-arrayed planar monopulse antennas," *IEEE Trans. Antennas Propag.*, vol. 57, no. 3, pp. 652-664, Mar. 2009
- [32] P. Rocca, L. Manica, A. Martini, and A. Massa, "Compromise sum-difference optimization through the iterative contiguous partition method," *IET Microwaves, Antennas & Propagation*, vol. 3, no. 2, pp. 348-361, 2009
- [33] L. Manica, P. Rocca, and A. Massa, "An excitation matching procedure for sub-arrayed monopulse arrays with maximum directivity," *IET Radar, Sonar & Navigation*, vol. 3, no. 1, pp. 42-48, Feb. 2009
- [34] L. Manica, P. Rocca, and A. Massa, "Design of subarrayed linear and planar array antennas with SLL control based on an excitation matching approach," *IEEE Trans. Antennas Propag.*, vol. 57, no. 6, pp. 1684-1691, Jun. 2009